

# Adaptive Unit Root Inference in Autoregressions using the Lasso Solution Path\*

Martin C. Arnold<sup>†</sup>

martin.arnold@vwl.uni-due.de

Thilo Reinschlüssel<sup>†‡</sup>

thilo.reinschluessel@vwl.uni-due.de

July 19, 2024

## **Abstract**

We show that the activation knot of a potentially non-stationary regressor on the adaptive Lasso solution path in autoregressions can be leveraged for selection-free inference about a unit root. The resulting test has asymptotic power against local alternatives in  $1/T$  neighbourhoods, unlike post-selection inference methods based on consistent model selection. Exploiting the information enrichment principle devised by Reinschlüssel and Arnold [arXiv:2402.16580, 2024] to improve the Lasso-based selection of ADF models, we propose a composite statistic and analyse its asymptotic distribution and local power function. Monte Carlo evidence shows that the combined test dominates the comparable post-selection inference methods of Tibshirani et al. [JASA, 2016, 514, 600–620] and may surpass the power of established unit root tests against local alternatives. We apply the new tests to groundwater level time series for Germany and find evidence rejecting stochastic trends to explain observed long-term declines in mean water levels.

**Keywords:** Adaptive Lasso, Time series, Unit root, Autoregressions, Local power

**JEL classifications:** C52, C22, C12

---

\*We thank Christoph Hanck for valuable comments that significantly improved the paper.

<sup>†</sup>Faculty of Business Administration and Economics, University of Duisburg-Essen, Universitätsstraße 12, 45117 Essen, Germany

<sup>‡</sup>RGS Econ - Ruhr Graduate School in Economics, Hohenzollernstraße 1-3, 45128 Essen, Germany

# 1 Introduction

Penalised estimators and their econometric applications have become increasingly important in recent decades. Many theoretical contributions are extensions of Lasso-type estimators (Fu & Knight, 2000), which go back to the seminal contribution of Tibshirani (1996). Despite their significant empirical relevance for economic disciplines such as macroeconomics and finance, methodological contributions to the penalised estimation of time series models are less frequent than for cross-section models. A majority of this research considers stationary time series. Examples which apply Lasso estimators to autoregressions are Wang et al. (2007), Hsu et al. (2008), Ren and Zhang (2010), and Medeiros and Mendes (2012). In high-dimensional settings, Hecq et al. (2023) address testing for Granger causality in vector autoregressions (VARs) using the concept of double-selection introduced by Belloni et al. (2013). Adamek et al. (2023) use the desparsified Lasso for inference in time series models with general error processes where the number of regressors may exceed the time dimension  $T$ .

Lasso-type estimators for time series models involving non-stationary data gain attention as well. One challenge here is to account for the different convergence rates of estimators when there are stationary and non-stationary regressors. For example, Liao and Phillips (2015) use Lasso-type regularisation for simultaneous selection of the cointegration rank and the lag order in vector error correction models. Koo et al. (2020) show the consistency of the Lasso in a high-dimensional predictive regression setup. Lee et al. (2022) propose using the adaptive Lasso in a double post-selection procedure for estimating predictive regressions with mixed-root regressors and multiple cointegration groups.

Caner and Knight (2013) show that Bridge estimators can be tuned for conservative model selection of augmented Dickey-Fuller (ADF) regressions. Kock (2016) proves that the adaptive Lasso (Zou, 2006) has the oracle property in ADF models and thus correctly selects the lag pattern and between stationary and non-stationary data  $y_t$  with probability approaching one as  $T \rightarrow \infty$ . These methods require tuning penalty functions to infer the order of integration from the estimated coefficient of the lagged level  $y_{t-1}$ .

We, in turn, suggest a tuning-free test for the adaptive Lasso to distinguish stationary and non-stationary autoregressions. The method exploits that the adaptive penalty weights drive the stochastic properties of knots on the Lasso solution path such that nuisance-parameter-free testing of the non-stationarity hypothesis is feasible. The only comparable approach we know of is post-selection inference with the spacing test by

Tibshirani et al. (2016) for sequential regression procedures that can be computed by a least angle regression (LAR) algorithm. Their idea is to test for zero partial correlation of a predictor with the LAR residual at its activation knot, adjusting for other variables currently in the active set. The null hypothesis of the spacing test is conditional on the inherently stochastic variable selection at a LAR knot. Our test differs from this approach since the null is unconditional on the remainder of the model, as we elaborate below.

Transferring the information enrichment principle of Arnold and Reinschlüssel (2023), we further suggest a combined test, enhancing the activation knot test with an auxiliary unit root test statistic via the penalty weight of  $y_{t-1}$ . We show that our tuning-free activation threshold tests have (asymptotic) power against local alternatives, contrary to the adaptive Lasso tuned for consistent model selection; see Theorem 5 in Kock (2016). Monte Carlo studies establish that the new tests are superior to the LAR post-selection methods of Lee et al. (2016) and Tibshirani et al. (2016, 2018). We further verify the usefulness of the principle by simulations, showing that the information-enriched test, in particular, closely tracks and may even outperform established unit root tests such as the nearly efficient ADF test of Elliott et al. (1996) under local alternatives.

The remainder of this article is as follows. Section 2 discusses the setup and recaps the estimation of autoregressions using the adaptive Lasso. In Section 3, we establish theoretical results on the solution path of the adaptive Lasso in ADF models underlying the new tests and discuss their implementation. Monte Carlo results are presented in Section 4. Section 5 illustrates the tests in an empirical application to German groundwater level time series. Section 6 concludes.

We will use the following conventions throughout the manuscript.  $\xrightarrow{p}$  and  $\xrightarrow{d}$  denote convergence in probability and distribution.  $\lambda = \Theta(T^\kappa)$  denotes  $0 < \liminf_{T \rightarrow \infty} \lambda/T^\kappa \leq \limsup_{T \rightarrow \infty} \lambda/T^\kappa < \infty$ ,  $\kappa \in \mathbb{R}$ .  $\|\mathbf{x}\|_q$  denotes the  $\ell_q$  norm of a vector  $\mathbf{x}$ . Coefficients of the data-generating model have a superscript  $\star$ . We refer to an estimator  $\widehat{\mathcal{M}}$  as model selection consistent if  $\lim_{T \rightarrow \infty} \mathbb{P}(\widehat{\mathcal{M}} = \mathcal{M}) = 1$  and conservative if  $\lim_{T \rightarrow \infty} \mathbb{P}(\widehat{\mathcal{M}} \supseteq \mathcal{M}) = 1$  with  $\lim_{T \rightarrow \infty} \mathbb{P}(\widehat{\mathcal{M}} \supset \mathcal{M}) > 0$ , where  $\mathcal{M} := \{i : \beta_i^\star \neq 0\}$  is the set of relevant variables. Several (estimated) quantities, often denoted by Greek symbols, depend on the  $\ell_1$  penalty and the sample size, which we express by sub-indexing with  $\lambda$  and  $T$  when helpful for the exposition. We define by  $\lambda_{\mathcal{O}}$  the continuum of sequences within a specific range of stochastic orders providing for the oracle property as  $T \rightarrow \infty$ . For ease of comprehension, we denote the set of sequences asymptotically leading to consistent ( $\lambda = \Theta(\lambda_{\mathcal{O}})$ ) or conservative ( $\lambda = o_p(\lambda_{\mathcal{O}})$ ) model selection by

$\lambda \in [0, \lambda_0]$ .

## 2 Adaptive Lasso estimation of autoregressions

This paper considers time series  $y_t$  with an autoregressive (AR) data-generating process (DGP) of the form

$$y_t = \mathbf{z}_t' \boldsymbol{\theta}^* + x_t, \quad x_t = \varrho^* x_{t-1} + u_t, \quad t = 1, \dots, T. \quad (1)$$

The process (1) incorporates a deterministic component  $\mathbf{z}_t = (1, t, \dots, t^q)'$  with coefficient vector  $\boldsymbol{\theta}^*$ , and a stochastic component  $x_t$  driven by the error process  $u_t$ . The stochastic component is a first-order AR process with parameter  $\varrho^*$ . We consider  $\varrho^* \in (-1, 1]$ , i.e.,  $x_t$  is stationary when  $|\varrho^*| < 1$  and non-stationary when  $\varrho^* = 1$ . The error process  $u_t$  satisfies the following assumptions.

**Assumption 1** (Linear process errors).  $u_t = \phi(L)\varepsilon_t$ , where the lag polynomial  $\phi(L)$  satisfies  $\phi(z) \neq 0$  for all  $|z| \leq 1$  and  $\sum_{j=1}^{\infty} j^s |\phi_j| < \infty$  for some  $s \geq 1$ . The innovations  $\varepsilon_t$  are a martingale difference sequence (MDS) such that  $E(\varepsilon_t^2) = \sigma^2$ ,  $T^{-1} \sum_t \varepsilon_t^2 \xrightarrow{p} \sigma^2$  and  $E|\varepsilon_t|^r < K_r$  with  $r \geq 4$  and some  $K_r < \infty$ .

Assumption 1 is adopted from Chang and Park (2002) and covers a general class of weakly stationary linear error processes, including ARMA processes with non-geometrically decaying coefficients. For the MDS innovations  $\varepsilon_t$  considered,  $u_t$  has ‘long-run’ variance (LRV)  $\omega^2 := \lim_{T \rightarrow \infty} E \left[ T^{-1} (\sum_{t=1}^T u_t)^2 \right] < \infty$ . Assumption 1 further ensures that  $u_t$  admits an AR( $\infty$ ) representation. Hence, the DGP (1) can be written as an ADF regression, i.e.,

$$\Delta y_t = d_t + \rho^* y_{t-1} + \sum_{j=1}^{\infty} \delta_j^* \Delta y_{t-j} + \varepsilon_t, \quad (2)$$

where  $d_t$  is a deterministic component,  $\rho^* \in (-2, 0]$ , and  $\sum_{j=1}^{\infty} \delta_j^* < 1$ .

Following Chang and Park (2002), we consider sparse approximations of (2),

$$\Delta y_t = d_t + \rho_p y_{t-1} + \sum_{j=1}^p \delta_{p,j} \Delta y_{t-j} + \varepsilon_{p,t}, \quad (3)$$

with lag order  $p$  suitably increasing as  $T \rightarrow \infty$ . Note that the coefficients  $\rho_p$  and  $\delta_{p,1}, \dots, \delta_{p,p}$  depend on the truncation lag  $p$  and are thus subject to approximation

errors  $\rho_p - \rho^*$  and  $\delta_{p,j} - \delta_j^*$ . The truncation additionally flaws the innovations with a truncation error  $\varepsilon_{p,t} - \varepsilon_t$ , cf. Remark 2.1 in Chang and Park (2002). All approximation errors and truncation errors vanish as  $p \rightarrow \infty$ .

**Assumption 2** (AR order).  $p$  satisfies  $p = o(T^{1/3})$  and  $p \rightarrow \infty$  as  $T \rightarrow \infty$ .

Chang and Park (2002) prove that under Assumption 2, ordinary least squares (OLS) estimation of (3) is consistent for all coefficients by eliminating the errors from approximation, truncation and estimation concurrently. They further show these conditions to suffice for the ADF t-ratio and the normalised coefficient statistic (Said and Dickey, 1984) to attain their respective limit distributions under the null hypothesis  $H_0: \rho^* = 0$ , as first studied in Dickey and Fuller (1979, 1981).

The adaptive Lasso (AL) estimator (Zou, 2006) in model (3) obtains as

$$\hat{\beta}_\lambda := (\hat{\rho}_\lambda, \hat{\delta}'_\lambda)' = \arg \min_{\dot{\rho}, \dot{\delta}} \Psi_T(\dot{\rho}, \dot{\delta}|\lambda), \quad (4)$$

where  $\Psi_T$  is the adaptively penalised loss function

$$\Psi_T(\dot{\rho}, \dot{\delta}|\lambda) := \sum_t \left( \Delta y_t - \dot{\rho} y_{t-1} - \sum_{j=1}^p \dot{\delta}_j \Delta y_{t-j} \right)^2 + 2\lambda \left( w_1^{\gamma_1} |\dot{\rho}| + \sum_{j=1}^p w_{2,j}^{\gamma_2} |\dot{\delta}_j| \right), \quad (5)$$

with  $\lambda \geq 0$  governing the  $\ell_1$  penalty, adaptive weights  $w_1 := 1/|\hat{\rho}|$ ,  $w_{2,j} := 1/|\hat{\delta}_j|$  determined by the initial OLS estimates  $\hat{\rho}$  and  $\hat{\delta}_j$ , and adjustment parameters  $\gamma_1, \gamma_2 \in \mathbb{R}^+$ . This loss function is equivalent to the one given in Kock (2016), except that we add a factor of 2 in front of the  $\ell_1$  penalty terms for mathematical convenience.

Kock (2016) shows that the AL solution (4) has the oracle property under suitable rate conditions for the  $\ell_1$  penalty parameter  $\lambda$ . Consequently, AL can select the relevant variables in (3) w.p. 1 as  $T \rightarrow \infty$  and consistently estimates their coefficients. This includes the decision whether  $y_{t-1}$  should be included in the model and, therefore, whether we have a stationary model with  $\rho^* \in (-2, 0)$  or the unit root case  $\rho^* = 0$ , so that  $y_{t-1}$  is excluded.

### 3 Testing for non-stationarity using the Lasso path

One central issue with inference in Lasso-type estimation is that conventional tests rely on marginal distributions, assuming fixed hypotheses. This inference is invalid for sequential regression estimators where solution paths are obtained from the LARS

algorithm (Efron et al., 2004): they do not account for the uncertainty about the model selected at a specific knot, rendering null hypotheses (typically stating the irrelevance of coefficients) in sub-models characterising the solution path random. This issue is crucial in testing for non-stationarity of autoregressions based on a solution to (5) where inference on the relevance of  $y_{t-1}$  depends on the selected lags.

A recent branch of the literature on step-wise estimators considers post-selection methods that address uncertainty about the selection in sequential regression, e.g., Lee et al. (2016) and Tibshirani et al. (2016, 2018). Their core result enables inference *conditional* on the stochastic variable selection using truncated Gaussian null distributions. Special cases of such tests are significance tests for a variable in the model selected at its LAR activation knot, i.e., just as the variable enters the set of active regressors.

We next show that a significance test for  $\rho^*$  in ADF regressions estimated by the adaptive Lasso can be derived immediately from the activation knot of  $y_{t-1}$  on the Lasso regularisation path. The new testing principle exploits two features of the AL solution. First, the (appropriately scaled) activation knot of *any irrelevant* regressor in (3) asymptotically follows a distribution that is independent of the set of regressors selected up to this knot, under consistent estimation of the coefficients. This allows identifying a nuisance-parameter-free limiting null distribution for  $\rho^* = 0$ . Second, the activation knots of the relevant regressors in (3) are of higher stochastic orders than those of the irrelevant regressors, which gives rise to the oracle property. This asymptotic sorting of activation knots allows the construction of consistent tests against the alternative  $\rho^* \in (-2, 0)$ .

### 3.1 An adaptive Lasso activation knot unit root test

Consider the LARS-computed sequence of penalty parameter values  $\lambda_1 > \lambda_2 > \dots > \lambda_K$  determining the regularisation path of the adaptive Lasso estimator (4). The knots  $\lambda_l$  are obtained from the corresponding Karush-Kuhn-Tucker conditions for a minimum of (5). Since variables are activated one at a time, the solution path features at least  $K = p + 1$  knots. The Lasso modification of the LARS algorithm may entail that the solution path also features knots where variables are *deactivated*. These variables are re-activated further down the solution path, resulting in  $K \geq p + 3$  in such cases.<sup>1</sup> Hereafter, we will be interested in the stochastic properties of a set of *activation knots* as specified by Definition 1.

---

<sup>1</sup>If a coefficient undergoes a sign change between activation knots, LAR in Lasso mode drops the variable and recomputes the OLS direction. See Section 3.1 in Efron et al. (2004) for details.

**Definition 1** (Activation knots). Let  $x_i \in (y_{t-1}, \Delta y_{t-1}, \dots, \Delta y_{t-p})'$ ,  $\dot{\beta} := (\dot{\rho}, \dot{\delta}')'$  and consider the coefficient functions  $\dot{\beta}_i(\lambda) \in \mathbb{R}$ ,  $i = 1, \dots, p+1$  along the adaptive Lasso solution path to (5). Define  $\lambda_{0, \beta_i^*}$  as the earliest activation knot of  $x_i$ , i.e.,

$$\begin{aligned} \lambda_{0, \beta_i^*} &:= \max \Lambda_{0, \beta_i^*}, \\ \Lambda_{0, \beta_i^*} &:= \left\{ \lambda : \partial_+ \dot{\beta}_i(\lambda) = 0 \quad \wedge \quad \partial_- \dot{\beta}_i(\lambda) \neq 0 \quad \wedge \quad \dot{\beta}_i(\lambda) = 0 \right\}, \end{aligned}$$

where  $\partial_+ \dot{\beta}_i(\lambda)$  and  $\partial_- \dot{\beta}_i(\lambda)$  denote derivatives of  $\dot{\beta}_i(\lambda)$  with respect to  $\lambda$  from above and from below, respectively.

The virtue of the adaptive Lasso is that the adaptive penalty weights  $w_1, w_{2,j}$ ,  $j = 1, \dots, p$  in (5) lead to distinct stochastic orders of the activation knots of a relevant ( $\lambda_{0, \beta_i^* \neq 0}$ ) and an irrelevant variable  $x_i$  ( $\lambda_{0, \beta_i^* = 0}$ ). These distinct orders give rise to tuning parameter sequences  $\lambda_{\mathcal{O}}$  satisfying the oracle conditions

$$\frac{\lambda_{\mathcal{O}}}{\sqrt{T}} \rightarrow 0, \quad \frac{\lambda_{\mathcal{O}}}{T^{1-\gamma_1}} \rightarrow \infty, \quad \frac{\lambda_{\mathcal{O}}}{T^{\frac{1-\gamma_2}{2}}} \rightarrow \infty, \quad (6)$$

requiring that  $\gamma_1 > 1/2$  and  $\gamma_2 > 0$  (Kock, 2016). In particular,  $\lambda_{\mathcal{O}}$  ensures consistent model selection. Since our aim is to distinguish stationary from non-stationary time series, we focus on the knots of  $y_{t-1}$ . We consider its first activation knot  $\lambda_{0, \rho^*}$  as stated in Definition 1 since it bears the most information regarding the shrinkage on the coefficient of  $y_{t-1}$ . We have

$$\lambda_{0, \rho^*} := w_1^{-\gamma_1} \left| \sum_t y_{t-1} \left( \Delta y_t - \sum_{j=1}^p \hat{\delta}_{\lambda, j} \Delta y_{t-j} \right) \right| \quad (7)$$

$$= w_1^{-\gamma_1} \left| \sum_t y_{t-1} \left( \rho^* y_{t-1} + \sum_{j=1}^p (\delta_j^* - \hat{\delta}_{\lambda, j}) \Delta y_{t-j} + \varepsilon_{p,t} \right) \right|, \quad (8)$$

where, by definition,  $\hat{\rho}_{\lambda} = 0$  for  $\lambda = \lambda_{0, \rho^*}$ . Based on  $\lambda_{0, \rho^*}$ , we propose a new route to classify stationary and non-stationary time series using the adaptive Lasso. The idea is to conduct inference on  $\rho^*$  using that the properly scaled activation knot  $\lambda_{0, \rho^*}$  is stochastically bounded under non-stationarity but diverges under stationarity as  $T \rightarrow \infty$ . In particular,

$$\lambda_{0, \rho^* = 0} = O_p \left( T^{1-\gamma_1} \right), \quad \text{and} \quad \lambda_{0, \rho^* \in (-2, 0)} = \Theta(T),$$

by Proposition 2 in Arnold and Reinschlüssel (2023). Consider  $H_0 : \rho^* = 0$  and  $H_1 :$

$\rho^* \in (-2, 0)$  and define  $\tau_{\gamma_1} := T^{\gamma_1-1} \lambda_{0, \rho^*}$ . Then,

$$\tau_{\gamma_1} | H_0 = O_p(1), \quad \text{and} \quad \tau_{\gamma_1} | H_1 = \Theta(T^{\gamma_1}),$$

which allows for right-sided testing of  $H_0$  against  $H_1$  using  $\tau_{\gamma_1}$ .

We next examine the anatomy of the statistic  $\tau_{\gamma_1}$  for non-stationary data and sketch its asymptotic null distribution  $F_{\tau_{\gamma_1}}$ . Under  $H_0 : \rho^* = 0$ , we use Eq. (8) to find

$$\tau_{\gamma_1} | H_0 = T^{\gamma_1-1} \left| \underbrace{\hat{\rho}}_{=: A_T} \right|^{\gamma_1} \left| \underbrace{\sum_t y_{t-1} \varepsilon_{p,t}}_{=: B_{T,\lambda}} + \underbrace{\sum_{j=1}^p (\delta_j^* - \hat{\delta}_{\lambda,j}) \sum_t y_{t-1} \Delta y_{t-j}}_{=: C_{T,\lambda}} \right| \quad (9)$$

$$= |T A_T|^{\gamma_1} \left| T^{-1} B_{T,\lambda} + T^{-1} C_{T,\lambda} \right|. \quad (10)$$

Note that  $T \cdot A_T = O_p(1)$  under Assumptions 1 and 2 as it is a continuous mapping of the unscaled Dickey-Fuller coefficient statistic  $T\hat{\rho}$ , cf. Chang and Park (2002). For identification of the limits of  $T^{-1}B_{T,\lambda}$  and  $T^{-1}C_{T,\lambda}$ , we require consistent coefficient estimates  $\hat{\beta}_\lambda$  for  $\lambda = \lambda_{0, \rho^*=0}$ : Consistency ensures  $\varepsilon_{p,t} \xrightarrow{p} \varepsilon_t$  so that  $T^{-1}B_{T,\lambda} = O_p(1)$  converges to a functional of a Brownian motion. Further, consistency of  $\hat{\beta}_\lambda$  implies the nuisance term  $T^{-1}C_{T,\lambda}$  to vanish asymptotically as  $\delta_j - \hat{\delta}_{\lambda,j} \xrightarrow{p} 0$ .

Because an oracle excludes any irrelevant variable, the activation knot of a unit root regressor  $y_{t-1}$  (with coefficient  $\rho^* = 0$ ) must satisfy

$$\liminf_{T \rightarrow \infty} \lambda_{0, \rho^*=0} = 0 \quad \text{and} \quad \limsup_{T \rightarrow \infty} \lambda_{0, \rho^*=0} \in [0, \lambda_{\mathcal{O}}]. \quad (11)$$

Therefore,  $\hat{\beta}_\lambda \xrightarrow{p} \beta^*$  for all  $\lambda = \lambda_{0, \rho^*=0}$  implies the existence of a distribution  $F_{\lambda_{0, \rho^*=0}}(\lambda)$  with all probability mass on the interval  $[0, \lambda_{\mathcal{O}}]$ . Scaling  $\lambda$  with  $T^{\gamma_1-1}$  delivers a stable and identifiable asymptotic null distribution  $F_{\tau_{\gamma_1}}$ ,

$$|T A_T|^{\gamma_1} \left| T^{-1} B_{T,\lambda} + o_p(1) \right| \stackrel{d}{\approx} F_{\tau_{\gamma_1}}(T^{\gamma_1-1} \lambda), \quad \lambda \in [0, \lambda_{\mathcal{O}}]. \quad (12)$$

Equation (12) states that  $F_{\tau_{\gamma_1}}$  is characterised by terms that solely hinge on  $w_1$ ,  $\gamma_1$  and the true innovations  $\varepsilon_t$ , and thus is independent of the unknown model  $\{\Delta y_{t-i} : i \in \mathcal{M}\}$ .

The gist of the new test is that selection of  $y_{t-1}$  rather than selection of the entire model avoids the need to tune  $\lambda$ : we may compute the solution path and select  $y_{t-1}$  if  $\tau_{\gamma_1} \geq T^{\gamma_1-1} \lambda_\alpha := F_{\tau_{\gamma_1}}^{-1}(1-\alpha)$ , i.e., *without* a data-driven choice of  $\lambda$ . In this regard, using  $\tau_{\gamma_1}$  for inference on whether  $\rho^* = 0$  is tuning-free but comes at the price of conservative



selection since  $\tau_{\gamma_1}$  selects an irrelevant  $y_{t-1}$  with fixed probability  $\alpha$  as  $T \rightarrow \infty$ . This is, however, inherent to classification using a significance test and may be attractive if the researcher wants to control the type-I-error rate. Another perspective is that  $\tau_{\gamma_1}$  provides inference on  $\rho^*$  that could be reported alongside a subsequently selected model.

**Remark 1.** Since  $\lambda_\alpha = o(\lambda_\phi)$  for any  $\alpha \in (0, 1]$ , setting  $\lambda = \lambda_\alpha$  in (4) yields tuning-free but conservative selection of *the whole model* (3).  $\hat{\beta}_{\lambda=\lambda_\alpha}$  could hence be an alternative to tuning  $\lambda$  for conservative selection, e.g., using the AIC. Both approaches ensure that  $\hat{\rho}_\lambda$  has asymptotic power against local alternatives  $\rho^* = O(T^{-1})$ . This contrasts consistent tuning where the adaptive Lasso has no asymptotic power against local alternatives in  $1/T$  neighbourhoods; see also Remark 3. A comparison of the AIC-tuned  $\hat{\beta}_\lambda$  with  $\hat{\beta}_{\lambda=\lambda_\alpha}$  under local alternatives would thus be interesting but is outside the scope of this paper.

We summarise the (local) asymptotic properties of  $\tau_{\gamma_1}$  for OLS weights in Theorem 1.

**Theorem 1.** *Consider model (3) with  $d_t = 0$  under Assumptions 1 and 2. Denote  $\lambda_{0,\rho^*}$  the activation threshold of  $y_{t-1}$  as in Definition 1 for some  $\gamma_1 > 1/2, \gamma_2 > 0$ , computed using the adaptive weights  $w_1 = |\hat{\rho}|^{-1}, w_{2,j} = |\hat{\delta}_j|^{-1}$ . Let  $\tau_{\gamma_1} := T^{\gamma_1-1}\lambda_{0,\rho^*}$ .*

1. *If  $\varrho^* = 1 + c/T$  for some  $c \in (-\infty, 0]$ , then*

$$\tau_{\gamma_1} \xrightarrow{d} \left| \phi(1)^{-1} \frac{W_c(1)^2 - 1}{2 \int_0^1 W_c(r)^2 dr} \right|^{\gamma_1} \left| \frac{1}{2} \sigma^2 \phi(1) (W_c(1)^2 - 1) \right|, \quad (13)$$

where  $W_c(r) := \int_0^r \exp[c(r-s)] dW(s)$  is an Ornstein-Uhlenbeck process driven by the standard Wiener process  $W(s)$  on  $s \in [0, 1]$ .

2. *If  $|\varrho^*| < 1$  is fixed, then  $\tau_{\gamma_1} = \Theta(T^{\gamma_1})$ .*

*Proof.* See Appendix A. ■

Part 1 of Theorem 1 states the limiting distribution of the (properly scaled) activation knot of  $y_{t-1}$  obtained from the LARS-computed solution path of the adaptive Lasso estimator considered in Kock (2016) in (near) unit root settings where  $\varrho^* = 1 + c/T$ . Setting  $c = 0$  obtains the null distribution under a unit root process. For  $-\infty < c < 0$ , Eq. (13) gives the limit of  $\tau_{\gamma_1}$  for stationary local deviations from the null. Result (13) shows the limiting distribution to depend on  $\gamma_1$ , which controls the impact of the adaptive weight  $w_1$ . The parameter  $\gamma_1$  thus governs the influence of the information about  $\rho^*$ , obtained from an auxiliary OLS regression. Part 2 of Theorem 1 states that  $\tau_{\gamma_1} \rightarrow \infty$  at rate  $T^{\gamma_1}$  under a fixed stationary alternative  $|\varrho^*| < 1$ .

**Remark 2.** An advantage over the tuned adaptive Lasso estimator  $\hat{\rho}_\lambda$  is that  $\tau_{\gamma_1}$  allows for inference with respect to  $\rho^* = 0$  using a tractable asymptotic distribution, as per Theorem 1. In contrast, the distributional properties of the adaptive Lasso are highly intricate. For cross-section models, Pötscher and Schneider (2009) show that finite-sample distributions may be highly non-standard and asymptotic (Gaussian) distributions provide poor approximations, even for large  $T$ . This issue is likely exacerbated by our potentially non-stationary time series setup. A thorough comparison of the tuned  $\hat{\rho}_\lambda$  to the  $\tau_{\gamma_1}$  test is an interesting point which is, however, beyond the scope of this paper.

**Remark 3.** In terms of correct selection probability,  $\hat{\rho}_\lambda$  is ‘blind’ for local alternatives  $\rho^* = O(1/T)$  if  $\lambda$  is tuned for consistent selection. This drawback of  $\hat{\rho}_\lambda$  is explicitly addressed by Kock (2016) for an AR(1) model with i.i.d. errors. Theorem 1 reveals that this result also applies to our generalised setting: for  $c \in (-\infty, 0]$ ,  $\lambda_{0, \rho^* \sim c/T} = o_p(\lambda_{\mathcal{O}})$ . Hence, under the local alternative  $\hat{\rho}_{\lambda=\lambda_{\mathcal{O}}} = 0$  w.p. 1 as  $T \rightarrow \infty$ , i.e.,  $y_{t-1}$  is asymptotically never activated at  $\lambda = \lambda_{\mathcal{O}}$ . In contrast,  $\tau_{\gamma_1}$  has asymptotic power against local alternatives, with the asymptotic power function depending on the limiting random variable in part 1 of Theorem 1. We investigate power against local alternatives in the Monte Carlo section.

### 3.2 Comparison with conditional post-selection inference for LARS fits

We next summarise the framework of Lee et al. (2016) and Tibshirani et al. (2016), review the LAR spacing test, and contrast the method with our testing concept. Consider the representative model

$$\mathbf{y} = \boldsymbol{\mu} + \boldsymbol{\epsilon}, \quad \boldsymbol{\epsilon} \sim N(\mathbf{0}, \boldsymbol{\Sigma}_T),$$

with fixed target  $\boldsymbol{\mu}$  so that  $\mathbf{y} \sim N(\boldsymbol{\mu}, \boldsymbol{\Sigma}_T)$  and  $\boldsymbol{\Sigma}_T$  is assumed to be known. Our interest is in making inferences about a linear functional  $\boldsymbol{\eta}'\boldsymbol{\mu}$ , where  $\boldsymbol{\eta} \in \mathbb{R}^T$  may depend on a selection event. Lee et al. (2016) and Tibshirani et al. (2016) show that a selection event on a LARS-computed solution path can be represented by a set of inequalities forming a polyhedral set  $\{\mathbf{y} : \mathbf{D}\mathbf{y} \leq \mathbf{b}\}$  defined by a matrix  $\mathbf{D}$  and a vector  $\mathbf{b}$ , where  $\leq$  is understood element-wise. Both papers paraphrase the same core result

**Lemma 1** (Polyhedral selection as truncation). *For any  $\boldsymbol{\Sigma}_T$ ,  $\boldsymbol{\eta}$  with  $\sigma_\eta^2 := \boldsymbol{\eta}'\boldsymbol{\Sigma}_T\boldsymbol{\eta} > 0$ ,*

$$\mathbf{D}\mathbf{y} \leq \mathbf{b} \iff \mathcal{V}^-(\mathbf{y}) \leq \boldsymbol{\eta}'\mathbf{y} \leq \mathcal{V}^+(\mathbf{y}), \mathcal{V}^0(\mathbf{y}) \geq 0,$$

where

$$\begin{aligned}\mathcal{V}^-(\mathbf{y}) &:= \max_{j:\alpha_j < 0} \frac{b_j - (\mathbf{D}\mathbf{y})_j + \alpha_j \boldsymbol{\eta}'\mathbf{y}}{\alpha_j}, \\ \mathcal{V}^+(\mathbf{y}) &:= \min_{j:\alpha_j > 0} \frac{b_j - (\mathbf{D}\mathbf{y})_j + \alpha_j \boldsymbol{\eta}'\mathbf{y}}{\alpha_j}, \\ \mathcal{V}^0(\mathbf{y}) &:= \min_{j:\alpha_j = 0} (b_j - (\mathbf{D}\mathbf{y})_j).\end{aligned}$$

and  $\boldsymbol{\alpha} := \mathbf{D}\boldsymbol{\Sigma}_T\boldsymbol{\eta}/\boldsymbol{\eta}'\boldsymbol{\Sigma}_T\boldsymbol{\eta}$ . The triplet  $(\mathcal{V}^-(\mathbf{y}), \mathcal{V}^+(\mathbf{y}), \mathcal{V}^0(\mathbf{y}))$  is independent of  $\boldsymbol{\eta}'\mathbf{y}$ .

*Proof.* See Lee et al. (2016) ■

Lemma 1 states that the selection event  $\{\mathbf{D}\mathbf{y} \leq \mathbf{b}\}$  is equivalent to  $\boldsymbol{\eta}'\mathbf{y}$  falling in the range  $\{\mathcal{V}^-(\mathbf{y}) \leq \boldsymbol{\eta}'\mathbf{y} \leq \mathcal{V}^+(\mathbf{y})\}$ . Inference conditional on selection can hence be conducted with the CDF of a  $N(\boldsymbol{\eta}'\boldsymbol{\mu}, \sigma_\eta^2)$  variable that is truncated to  $[\mathcal{V}^-(\mathbf{y}), \mathcal{V}^+(\mathbf{y})]$ ,

$$F_{\boldsymbol{\eta}'\boldsymbol{\mu}, \sigma_\eta^2}^{[\mathcal{V}^-(\mathbf{y}), \mathcal{V}^+(\mathbf{y})]}(x) := \frac{\Phi((x - \boldsymbol{\eta}'\boldsymbol{\mu})/\sigma_\eta) - \Phi((\mathcal{V}^-(\mathbf{y}) - \boldsymbol{\eta}'\boldsymbol{\mu})/\sigma_\eta)}{\Phi((\mathcal{V}^+(\mathbf{y}) - \boldsymbol{\eta}'\boldsymbol{\mu})/\sigma_\eta) - \Phi((\mathcal{V}^-(\mathbf{y}) - \boldsymbol{\eta}'\boldsymbol{\mu})/\sigma_\eta)}, \quad (14)$$

using the transform

$$F_{\boldsymbol{\eta}'\boldsymbol{\mu}, \sigma_\eta^2}^{[\mathcal{V}^-(\mathbf{y}), \mathcal{V}^+(\mathbf{y})]}(\boldsymbol{\eta}'\mathbf{y}) \mid \{\mathbf{D}\mathbf{y} \leq \mathbf{b}\} \sim U(0, 1), \quad (15)$$

with  $U(0, 1)$  the standard uniform distribution. Tibshirani et al. (2016) discuss several tests based on (15). A test statistic for

$$H_0 : \boldsymbol{\eta}'\boldsymbol{\mu} = 0 \quad \text{vs.} \quad H_1 : \boldsymbol{\eta}'\boldsymbol{\mu} \neq 0 \quad (16)$$

is the marginal significance level

$$\mathcal{TG} = 2 \cdot \min \left\{ F_{0, \sigma_\eta^2}^{[\mathcal{V}^-(\mathbf{y}), \mathcal{V}^+(\mathbf{y})]}(\boldsymbol{\eta}'\mathbf{y}), 1 - F_{0, \sigma_\eta^2}^{[\mathcal{V}^-(\mathbf{y}), \mathcal{V}^+(\mathbf{y})]}(\boldsymbol{\eta}'\mathbf{y}) \right\}. \quad (17)$$

Using  $\mathcal{TG}$  as a p-value gives an exact level- $\alpha$ -test under the above-mentioned conditions.

For  $\boldsymbol{\mu} = \mathbf{X}\boldsymbol{\beta}^*$  result (17) is the p-value for a test of linear constraints on the coefficients  $\boldsymbol{\beta}$ , conditional on a selection event on a LARS solution path corresponding to some fixed value for the regularisation parameter  $\lambda$ . Denote  $\mathbf{X}_{\mathcal{A}_\lambda} \in \mathbb{R}^{T \times |\mathcal{A}_\lambda|}$  the sub-matrix of  $\mathbf{X} \in \mathbb{R}^{p+1}$  containing the active variables at  $\lambda$  with the index set  $\mathcal{A}_\lambda \subset \{1, \dots, p+1\}$ . An interesting specification is  $\boldsymbol{\eta} = (\mathbf{X}_{\mathcal{A}_\lambda}^+)' \mathbf{e}_j$ ,  $j \in \mathcal{A}_\lambda$  with  $\mathbf{X}_{\mathcal{A}_\lambda}^+ := (\mathbf{X}_{\mathcal{A}_\lambda}' \mathbf{X}_{\mathcal{A}_\lambda})^{-1} \mathbf{X}_{\mathcal{A}_\lambda}'$

and  $\mathbf{e}_j$  the suitable  $j^{\text{th}}$  standard basis vector. Using  $\mathcal{TG}$ , we may test

$$H_0 : \boldsymbol{\eta}'\boldsymbol{\mu} = \mathbf{e}'_j(\mathbf{X}'_{\mathcal{A}_\lambda}\mathbf{X}_{\mathcal{A}_\lambda})^{-1}\mathbf{X}'_{\mathcal{A}_\lambda}\mathbf{X}\boldsymbol{\beta}^* = 0, \quad \text{vs.} \quad H_1 : \boldsymbol{\eta}'\boldsymbol{\mu} \neq 0, \quad (18)$$

i.e., the significance of the partial regression coefficient of variable  $j$  in the projected linear model of  $\boldsymbol{\mu} = \mathbf{X}\boldsymbol{\beta}^*$  on  $\mathbf{X}_{\mathcal{A}_\lambda}$ , conditional on the random selection  $\mathcal{A}_\lambda$  at  $\lambda$ .

Tibshirani et al. (2016) suggest a special test based on the polyhedral set representation of selection events for LAR that has similarities with our activation knot tests. Their theory considers the active set  $\mathcal{A}_l$  at  $\lambda = \lambda_l$ , the  $l^{\text{th}}$  step of LAR. Denote  $\mathbf{x}_{j_l}$  the variable *entering*  $\mathcal{A}_l$  at step  $l$ . They suggest setting  $\boldsymbol{\eta}_l := (\mathbf{X}_{\mathcal{A}_l}^+)' \mathbf{e}_j$  and to test  $\boldsymbol{\eta}'_l \boldsymbol{\mu} = 0$  against  $\boldsymbol{\eta}'_l \boldsymbol{\mu} > 0$ , which is

$$H_0 : \mathbf{e}'_j \mathbf{X}_{\mathcal{A}_l}^+ \boldsymbol{\mu} = 0 \quad \text{vs.} \quad H_1 : \text{sgn} \left( \mathbf{e}'_j \mathbf{X}_{\mathcal{A}_l}^+ \mathbf{y} \right) \cdot \mathbf{e}'_j \mathbf{X}_{\mathcal{A}_l}^+ \boldsymbol{\mu} > 0. \quad (19)$$

Testing  $H_0 : \boldsymbol{\eta}'_l \boldsymbol{\mu} = 0$  amounts to testing the variable entering the active set at the  $l^{\text{th}}$  LARS step to have zero partial regression coefficient  $\mathbf{e}'_j \mathbf{X}_{\mathcal{A}_l}^+ \boldsymbol{\mu}$  against the alternative that the coefficient is non-zero and has the same sign as the sample regression coefficient  $\mathbf{e}'_j \mathbf{X}_{\mathcal{A}_l}^+ \mathbf{y}$ .

Tibshirani et al. (2016) add the restriction  $\boldsymbol{\Sigma}_T = \sigma^2 \mathbf{I}_T$  to devise the feasible statistic

$$\mathcal{S} := \frac{\Phi \left( \lambda_{l-1} \frac{\nu_l}{\sigma} \right) - \Phi \left( \lambda_l \frac{\nu_l}{\sigma} \right)}{\Phi \left( \lambda_{l-1} \frac{\nu_l}{\sigma} \right) - \Phi \left( \lambda_{l+1} \frac{\nu_l}{\sigma} \right)}, \quad (20)$$

which is based on an approximate representation of the selection event at step  $l$ , where

$$\nu_l := \left\| (\mathbf{X}_{\mathcal{A}_l}^+)' \mathbf{s}_{\mathcal{A}_l} - (\mathbf{X}_{\mathcal{A}_{l-1}}^+)' \mathbf{s}_{\mathcal{A}_{l-1}} \right\|_2,$$

and  $\mathbf{s}_{\mathcal{A}_l}$  is the sign vector of the active variables at step  $l$ , see Theorem 2 of Tibshirani et al. (2016).  $\mathcal{S}$  decreases monotonically in  $\lambda_l - \lambda_{l+1} > 0$  and tests for an insignificant spacing between the LAR activation knots  $\lambda_l$  and  $\lambda_{l+1}$ , and is hence called the *spacing test* for LAR. We stress that  $\mathcal{S}$  is not readily applicable to time series regressions due to the restriction of a spherical  $\boldsymbol{\Sigma}_T$ .

Tibshirani et al. (2018) relax the rigid assumption of Gaussian errors towards a broad class of error distributions for which they prove the  $\mathcal{TG}$ -type statistics to remain pivotal in low-dimensional ( $p < T$ ) cases. They also propose a plug-in estimator for  $\sigma^2$  and provide simulation evidence for the validity of their asymptotic results in broader settings like heteroskedastic errors.

The above exposition shows how the underlying principles of  $\tau_{\gamma_1}$  and  $\mathcal{S}$  differ in testing the relevance of  $y_{t-1}$  in ADF regressions:  $\mathcal{S}$  tests whether the partial regression coefficient of  $y_{t-1}$  is zero in a regression of  $\Delta y_t$  on  $y_{t-1}$  and the set of the  $\Delta y_{t-j}$ ,  $j \in \mathcal{A}_l$  at  $\lambda_l = \lambda_{0, \rho^*}^{\text{LAR}}$ , the LAR activation knot of  $y_{t-1}$ . The inference is *conditional* on a randomly selected lag structure and is approximate for  $T < \infty$  in non-Gaussian settings.  $\mathcal{S}$  rejects the null of irrelevance of  $y_{t-1}$  in a model with regressors  $\mathbf{X}_{\mathcal{A}_l}$  for a significant difference  $\lambda_l - \lambda_{l+1}$ . Hence  $\mathcal{S}$  places its level- $\alpha$  critical value somewhere between  $\lambda_{l-1}$  and  $\lambda_{l+1}$ , rendering the critical region data-dependent.

In contrast,  $\tau_{\gamma_1}$  compares the scaled LARS-computed adaptive Lasso activation knot  $\lambda_{0, \rho^*}$  with a pre-determined quantile  $\lambda_{c_\alpha}$  of its *marginal* asymptotic distribution in a non-stationary model. If the *stochastic order* of  $\lambda_{0, \rho^*}$  is larger than expected under non-stationarity, the activation knot  $\lambda_{0, \rho^*}$  eventually exceeds the fixed critical value  $\lambda_\alpha$ , causing  $\tau_{\gamma_1}$  to reject the null hypothesis of  $y_{t-1}$  being an irrelevant regressor. The property  $\lambda_{0, \rho^*=0} = o_p(\lambda_\mathcal{O})$  ensures that the selected model at  $\lambda = \lambda_{0, \rho^*=0}$  contains the true model w.p. 1 as  $T \rightarrow \infty$  under  $H_0$ , akin to the *screening property* in Meinshausen et al. (2009). Consistency implies the potential extra regressors do not impact the asymptotic distribution of  $\lambda_{0, \rho^*}$ , as stated in Theorem 1. Therefore, finite-sample inference based on  $\tau_{\gamma_1}$  is also approximate but is *unconditional* on the stochastic variable selection at  $\lambda = \lambda_{0, \rho^*=0}$ .

Since LAR is a greedy algorithm, it is complicated to assess the usefulness of the spacing test analytically, especially in time series models with stochastic regressors. However, as the solution path of LAR is similar to that of the inconsistent plain (non-adaptive) Lasso, penalising non-zero parameters in ADF regressions even as  $T \rightarrow \infty$  (see Kock (2016), Theorem 7), we expect poor performance of LAR as well.<sup>2</sup> To investigate the performance of the spacing test for solution paths similar to those of a consistent adaptive Lasso estimator, we consider a variant of LAR based on regressors that are weighted as implied by (5) in the Monte Carlo section. We refer to this estimator as *adaptive LAR*, implemented like the adaptive Lasso but using the LARS algorithm in LAR mode.

**Remark 4.** Notably, the adaptive LAR features the oracle property, placing both  $\lambda_{0, \rho^*}^{\text{LAR}}$  and the spacing test's critical value  $\lambda_\alpha^{\mathcal{S}}$  below  $\lambda_\mathcal{O}$  as  $T \rightarrow \infty$ . By consistency of the coefficient estimators in this interval on the solution path, the true innovations  $\varepsilon_t$  are asymptotically recovered and meet the fundamental condition  $\boldsymbol{\epsilon} \sim (\mathbf{0}, \sigma^2 \mathbf{I}_T)$ . Relaxing

---

<sup>2</sup>Simulation results in Arnold and Reinschlüssel (2023) confirm the erratic performance of the BIC-tuned plain Lasso in ADF regressions.

the MDS condition on  $\varepsilon_t$  in Assumption 1 to independence ensures that all conditions for the spacing test are asymptotically satisfied at  $\lambda_\alpha^S$ . Therefore, we conjecture that the spacing test applied to the *adaptive* LAR is asymptotically valid in similar applications which violate the conditions on  $\Sigma_T$  for the original LAR-based test. We revisit this point in the Monte Carlo section.

### 3.3 An enhanced test using auxiliary information

In Arnold and Reinschlüssel (2023), we suggest a modified weight for  $y_{t-1}$  in the adaptive Lasso estimator (3) that aims for improved discrimination between stationary and non-stationary models under (consistent) tuning of  $\lambda$ . The idea is to enhance the adaptive weight  $w_1$  with additional information on  $\rho^*$ : the enriched weight  $\check{w}_1 = |\hat{\rho}/J_\alpha|^{-1}$  scales  $w_1$  by a simulated statistic  $J_\alpha$  which exploits different orders in probability in balanced and unbalanced regressions.<sup>3</sup> The merits of information enrichment result from the stochastic order of the corresponding  $\lambda_0$ , denoted  $\check{\lambda}_{0,\rho^*}$ . The key is that both  $\lambda_{0,\rho^*}$  and  $\check{\lambda}_{0,\rho^*}$  are  $O_p(T^{1-\gamma_1})$  under non-stationarity, but for fixed stationary alternatives  $\rho^* \in (-2, 0)$ ,

$$\lambda_{0,\rho^* \in (-2,0)} = o\left(\check{\lambda}_{0,\rho^* \in (-2,0)}\right),$$

implying beneficial properties for the resulting information-enriched adaptive Lasso estimator (ALIE). In particular, we demonstrate that ALIE has higher power under consistent tuning. Our simulation evidence also indicates that  $\check{w}_1$  improves on the simple OLS-based weight regarding the activation rate of  $y_{t-1}$  in small samples when  $\rho^* = 0$ .

It is possible to transfer these benefits to the  $\tau_{\gamma_1}$  test if computed using  $\check{w}_1$  instead of  $w_1$ . We summarise properties of the resulting modified test statistic, denoted  $\check{\tau}_{\gamma_1}$ , in the following corollary to Theorem 1.

**Corollary 1.** *Consider the assumptions of Theorem 1. Denote  $\check{\lambda}_{0,\rho^*}$  the activation threshold of  $y_{t-1}$  as in Definition 1, computed using the adaptive weights  $\check{w}_1 = |\hat{\rho}/J_\alpha|^{-1}$  and  $w_{2,j} = |\hat{\delta}_j|^{-1}$  for  $\gamma_1 > 1/2$ ,  $\gamma_2 > 0$ . Let  $\check{\tau}_{\gamma_1} := T^{\gamma_1-1}\check{\lambda}_{0,\rho^*}$ .*

1. *If  $\varrho^* = 1 + c/T$  for some  $c \in (-\infty, 0]$ , then*

$$\check{\tau}_{\gamma_1} = \frac{\tau_{\gamma_1}}{J_\alpha^{\gamma_1}} \xrightarrow{d} \frac{1}{J_{\alpha,c}^{\gamma_1}} \left| \phi(1)^{-1} \frac{W_c(1)^2 - 1}{2 \int_0^1 W_c(r)^2 dr} \right|^{\gamma_1} \left| \frac{1}{2} \sigma^2 \phi(1) (W_c(1)^2 - 1) \right|,$$

---

<sup>3</sup>See Herwartz and Siedenburg (2010) for details on  $J_\alpha$ . See Algorithm 1 in Appendix B for details on the computation of  $\check{w}_1$ .

where  $J_{\alpha,c}$  denotes the  $c$ -dependent weak limit of  $J_\alpha$ . All other quantities are defined in Theorem 1.

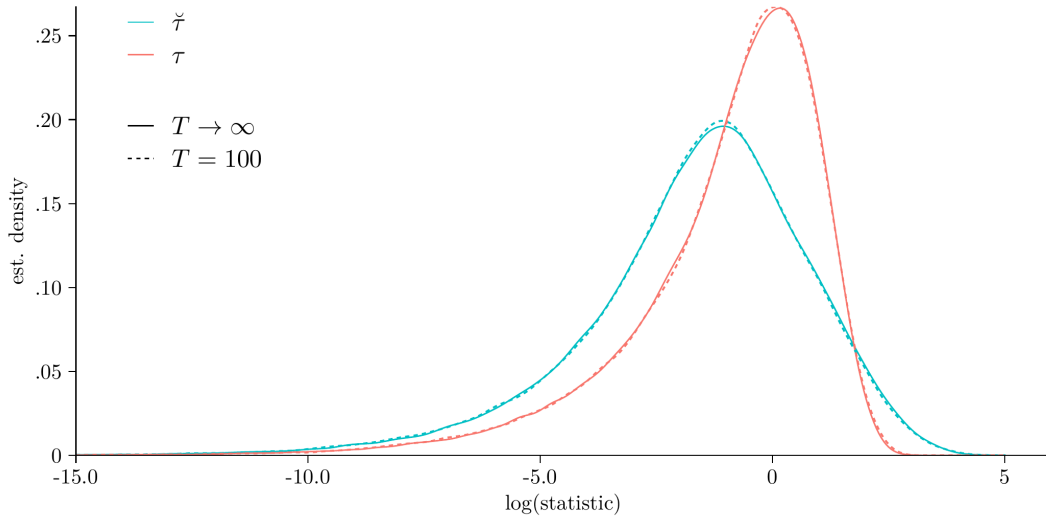
2. If  $|\varrho^*| < 1$  is fixed, then  $\check{\tau}_{\gamma_1} = \Theta(T^{2\gamma_1})$ .

*Proof.* See Appendix A. ■

Corollary 1 shows how the information-enriched adaptive weight suggested in Arnold and Reinschlüssel (2023) alters the asymptotic distribution of the scaled activation knot of  $y_{t-1}$ . Part 1 of Corollary 1 states that  $\check{\tau}_{\gamma_1} = \tau_{\gamma_1}/J_\alpha^{\gamma_1}$  and so the modified weight  $\check{w}_1$  results in a scaling of the limiting random variable in part 1 of Theorem 1 under non-stationarity or local alternatives. From Part 2 of Corollary 1, we deduce that  $\check{\tau}_{\gamma_1}$  diverges with the squared rate of  $\tau_{\gamma_1}$  under a fixed stationary alternative, suggesting a power advantage through information enrichment for all admissible choices of  $\gamma_1$ .

### 3.4 Implementation

Figure 1: Simulated null distributions of the adaptive Lasso activation knot tests



*Notes:* Gaussian KDEs on the natural log scale using the Silverman (1986) rule. Dashed lines show finite-sample distributions for DGP (1) with  $\theta = 0$ ,  $\varrho = 1$ , and  $u_t \sim i.i.d. N(0, 1)$ .  $\lambda_{0,\rho^*}$  and  $\check{\lambda}_{0,\rho^*}$  are taken from the `lars` computed solution path for the adaptive Lasso with  $\gamma_1 = \gamma_2 = 1$  in model (3). Asymptotic distributions (solid lines) are computed using discrete approximations of the limiting r.v.s in (21) for  $10^4$  steps and with  $\sigma^2 = 1$ .  $10^5$  replications.

Computing the Lasso solution path for (5) is straightforward, e.g., using the `lars` package (Hastie & Efron, 2022) for the statistical programming language R (R Core Team,

2023). The tests generally require choosing  $\gamma_1$  and accommodation for the LRV component  $\sigma^2\phi(1)$  to obtain nuisance-parameter free limit distributions. A common choice in applications of the adaptive Lasso is  $\gamma_1 = \gamma_2 = 1$ . This is convenient, since then

$$\tau_{\gamma_1=1} \xrightarrow{d} \sigma^2 \frac{(W_c(1)^2 - 1)^2}{4 \int_0^1 W_c(r)^2 dr}, \quad \check{\tau}_{\gamma_1=1} \xrightarrow{d} \frac{\sigma^2}{J_{\alpha,c}} \frac{(W_c(1)^2 - 1)^2}{4 \int_0^1 W_c(r)^2 dr}, \quad (21)$$

by part 1 of Theorem 1 and Corollary 1, respectively. Notably, the limiting random variables in (21) do not depend on  $\phi(1)$  and thus, the asymptotic impact of the error process  $u_t$  reduces to scaling by the innovation variance  $\sigma^2$ . Hence, we only need to adjust for  $\sigma^2$  to obtain nuisance-parameter-free limit distributions. For consistent estimation of  $\sigma^2$  we suggest using

$$\hat{\sigma}^2 := \frac{1}{T - p - 1} \sum_t \hat{\varepsilon}_{p,t}^2, \quad (22)$$

where the  $\hat{\varepsilon}_{p,t}$  are residuals from the auxiliary ADF( $p$ ) regression for computing the penalty weights. We henceforth refer to these test statistics as  $\tau := \tau_{\gamma_1=1}/\hat{\sigma}^2$  and  $\check{\tau} := \check{\tau}_{\gamma_1=1}/\hat{\sigma}^2$ .

Kernel density estimates (KDEs) of the asymptotic null distributions of  $\tau$  and  $\check{\tau}$  for  $c = 0$  are shown (by the solid lines) in Figure 1. Given the high kurtosis of the distributions, we transform the simulated statistics to the natural log scale for ease of interpretation. We compare these with KDEs of the sample distributions for  $T = 100$  in a non-stationary ADF model with  $p = 0$ . Both limit distributions seem well approximated by their corresponding finite-sample distribution for  $p = 0$ . Simulated critical values of  $\tau$  and  $\check{\tau}$  are presented in Table 1.

### 3.5 Deterministic components

While we so far assumed that  $d_t = 0$ , it is interesting to consider empirically relevant scenarios where the DGP is allowed to include a constant term or a linear time trend. Following Arnold and Reinschlüssel (2023), we consider first-difference detrending (FD), see Schmidt and Phillips (1992). While adjusting for a constant by FD does not affect the limiting random variable of  $\tau$  in (21), the trend-adjusted data are

$$y_t^{\text{FD}} := y_t - y_1 - \frac{t}{T}(y_T - y_1)$$



Table 1: Simulated critical values of adaptive Lasso activation knot tests

$T$	$\tau$			$\check{\tau}$		
	1%	5%	10%	1%	5%	10%
50	7.43	4.30	3.07	15.87	5.73	3.06
75	7.23	4.22	3.03	15.94	5.81	3.11
100	7.18	4.23	3.03	16.55	5.93	3.15
150	7.06	4.18	3.00	16.32	5.94	3.17
250	7.03	4.15	2.99	16.60	5.98	3.20
500	7.00	4.13	2.97	16.65	6.01	3.20
1000	6.97	4.13	2.97	16.78	6.04	3.22

*Notes:* Critical values are computed based on the adaptive Lasso solution to (3) with  $d_t = 0$  and  $p = 0$  for Gaussian random walks.  $\check{\tau}$  is computed using  $J_\alpha$  with  $\alpha = .1$  and  $\sigma^2$  estimated by  $\hat{\sigma}^2$ .  $5 \cdot 10^5$  replications.

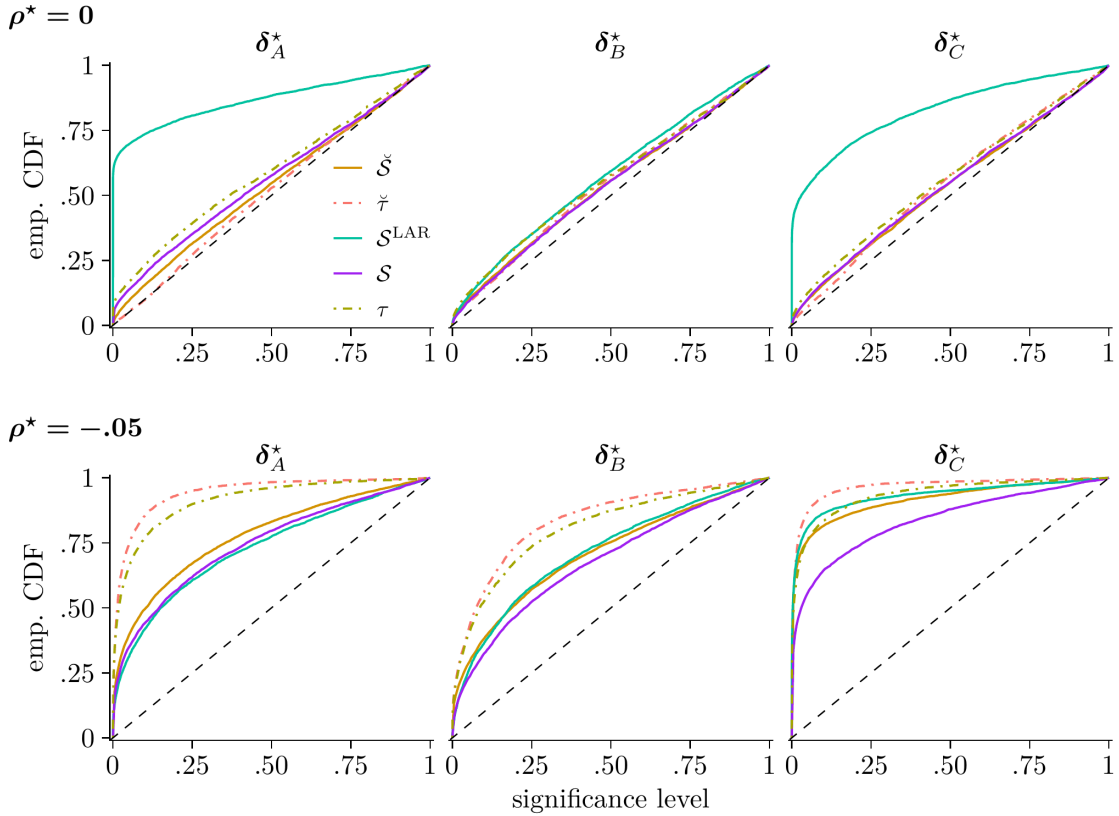
which results in  $W_c(r)$  being replaced by  $V(r) := W_c(r) - rW_c(1)$ . The latter carries over to the limit of  $\check{\tau}$ . Note that the limit of  $\check{\tau}$  is altered under demeaning as well since  $J_\alpha$  is computed using OLS regressions adjusting for deterministic components, see Algorithm 1 in Appendix B. We provide simulated finite-sample critical values for statistics computed on adjusted data in Table D1. We investigate performance under detrending in the Monte Carlo studies in Section 4.2.

## 4 Monte Carlo evidence

We next present two simulation studies. In Section 4.1, we compare methods for inference on  $\rho^* = 0$  using the knots on LARS-computed solution paths. Besides the new tests  $\tau$  and  $\check{\tau}$ , we consider the spacing test for plain and adaptive LAR, and the adaptive Lasso estimator from Kock (2016) tuned with BIC for consistent model selection ( $AL_{BIC}$ ), as well as its information-enriched version ( $ALIE_{BIC}$ ) introduced in Arnold and Reinschlüssel (2023).

We consider AR DGPs where  $|\mathcal{M}| < \infty$  so that selecting all relevant variables is feasible for  $T < \infty$ . Such a setting is useful in several regards. First, our theoretical results in Section 3 suggest that the finite- $T$  performance of  $\tau$  and  $\check{\tau}$  hinges on  $\widehat{\mathcal{M}} \supseteq \mathcal{M}$ , i.e., the selection of the all relevant variables, at  $\lambda_{0,\rho^*}$  and  $\check{\lambda}_{0,\rho^*}$  in conjunction with sufficient shrinkage of the coefficients of irrelevant variables. A similar reasoning applies to  $AL_{BIC}$  and  $ALIE_{BIC}$  at  $\lambda_{BIC}$ . Second, finite-order AR models allow us to investigate our conjecture from Remark 4 that the spacing tests deliver asymptotically valid inference when applied to *adaptive* LAR in ADF models that can be consistently

Figure 2: Empirical CDFs of p-values for activation knot tests



Notes: DGP (23) with  $T = 75$ .  $\delta_A^* = (.4, .3, .2, 0, 0, 0, -.2, 0, 0, .2)'$ ,  $\delta_B^* = (-.4, 0, 7)$ , and  $\delta_C^* = .8$ . Curves show empirical CDFs of observed p-values. The dashed lines reference an expected  $U(0,1)$  CDF under  $H_0$ . Model (3) with  $d_t = 0$  and  $p = 10$ . 5000 replications.

estimated, contrary to the (plain) LAR spacing test of Tibshirani et al. (2016). Another aspect of the study is to gauge the improvement information enrichment provides for the testing paradigm of the spacing test.

Given the apparent relation of the proposed activation knot tests to methods based on unpenalised OLS estimation of model (3), Section 4.2 investigates how  $\tau$  and  $\check{\tau}$  rank among established unit root tests in terms of asymptotic efficiency. For this, we assess the methods' local power properties in a near-integration framework where  $\varrho = c/T$ ,  $c \in (-\infty, 0]$ . As benchmarks, we consider the augmented Dickey-Fuller t-statistic  $ADF^{\text{GLS}}$  of Elliott et al. (1996), the modified Phillips-Perron statistic  $MZ_t$  by Ng and Perron (2001) and the  $J_\alpha$  statistic of Herwartz and Siedenbueg (2010) used in computing  $\check{\tau}$ .

## 4.1 Comparison with selection-based inference

We generate the data using the recursion

$$y_t(1 - B(L)) = v_t, \quad v_t \stackrel{i.i.d.}{\sim} N(0, 1), \quad t = 1, \dots, T + 50, \quad (23)$$

with

$$B(L) = (\rho^* + \delta_1^*)L + (\delta_2^* - \delta_1^*)L^2 + \dots + (\delta_{k^*-1}^* - \delta_{k^*}^*)L^{k^*} - \delta_{k^*}^*L^{k^*+1},$$

and  $k^* + 1$  zero initial values where  $k^* := \dim(\boldsymbol{\delta}^*)$ . The first 50 samples are discarded. DGP (23) has an ADF representation with coefficients  $(\rho^*, \boldsymbol{\delta}^*)'$ . We distinguish between the unit root case  $\rho^* = 0$  and the fixed alternative  $\rho^* = -.05$ . Three different configurations of  $\boldsymbol{\delta}^*$  are considered: we assess the performance for a challenging sparsity pattern using  $\boldsymbol{\delta}_A^* := (.4, .3, .2, 0, 0, 0, -.2, 0, .2)'$ .  $\boldsymbol{\delta}_B^* := (-.4, 0, .7)'$  is a low power setting for unit root tests, and  $\boldsymbol{\delta}_C^* := .8$  yields a short AR process with slowly decaying auto-correlation. These settings are used in Arnold and Reinschlüssel (2023) to compare BIC-tuned adaptive Lasso estimators based on  $w_1$  or  $\check{w}_1$  in their ability to discriminate stationary and non-stationary data.

The LAR spacing test  $\mathcal{S}^{\text{LAR}}$  as defined in (20), termed the *modified spacing test*, is computed with the `selectiveInference` R package (Tibshirani et al., 2019). We further report the adaptive LAR variants suggested in Remark 4 based on OLS-only weights ( $\mathcal{S}$ ) and with the information-enriched weight  $\check{w}_1$  for  $y_{t-1}$  ( $\check{\mathcal{S}}$ ). These are computed by the same algorithm as  $\mathcal{S}^{\text{LAR}}$  but follow from LAR estimates based on the scaled regressors

$$\tilde{\mathbf{X}} := \left( w_1^{-\gamma_1} \mathbf{y}_{t-1}, w_{2,1}^{-\gamma_2} \Delta \mathbf{y}_{t-1}, \dots, w_{2,p}^{-\gamma_2} \Delta \mathbf{y}_{t-p} \right).$$

To implement the spacing tests, we estimate  $\sigma^2$  by Eq. (22) using OLS residuals from the ADF regression for computing the penalty weights.

We first simulate data for  $T = 75$ , a usual sample size in macroeconomic applications, and estimate model (3) with fixed lag length  $p = 10$  and  $d_t = 0$ . Figure 2 compares the empirical CDFs of the p-values with the reference quantiles of a standard uniform distribution under  $H_0$ . All tests are somewhat anti-conservative under the null (top panel) in all scenarios. Outcomes indicate that the finite-sample distribution of  $\mathcal{S}^{\text{LAR}}$  is a poor approximation of the  $U(0, 1)$  distribution and may entail unacceptable upward size distortions. This observation is consistent with the theory behind the spacing test ruling out serial correlation in the dependent variable. An exception is  $\boldsymbol{\delta}_B^*$  where

$\mathcal{S}^{\text{LAR}}$  performs comparably to the other tests. Differences among the latter are most pronounced for  $\delta_A^*$ , where  $\tau$  performs worst, followed by the spacing tests for adaptive LAR. The information-enriched statistic  $\check{\tau}$  performs best here and has an almost exact size for typical significance levels.

Corroborating Remark 4, the results show that the adaptive LAR tests  $\mathcal{S}$  and  $\check{\mathcal{S}}$  perform much better than  $\mathcal{S}^{\text{LAR}}$  as their empirical distributions for  $\delta_A^*$  and  $\delta_C^*$  are more closely approximated by the theoretical null distributions than  $\tau$ . Furthermore, we find that  $\check{w}_1$  mitigates the size distortions of  $\check{\mathcal{S}}$  compared to  $\mathcal{S}$ , a direct effect of information enrichment.

All methods have power under the alternative (bottom panel), as indicated by empirical CDFs well above the dashed 45° line. We again observe a positive effect of information enrichment for the adaptive LAR spacing tests, leading to a higher power of  $\check{\mathcal{S}}$  than  $\mathcal{S}$ , which is most pronounced for  $\delta_C^*$ . Analogous outcomes are seen for  $\check{\tau}$  and  $\tau$ . In particular, the comparison with the null results suggests that methods based on the modified penalty weight are superior. Furthermore, the discrepancies in CDFs are strong evidence that the adaptive Lasso activation threshold tests, especially  $\check{\tau}$ , have higher power than the spacing tests.

Table 2 provides a detailed comparison of the tests at 5% for sample sizes  $T \in \{50, 75, 100, 150, 250, 500\}$ . We additionally report outcomes for  $\text{AL}_{\text{BIC}}$  and  $\text{ALIE}_{\text{BIC}}$ . Results for non-stationary data (top panel) confirm the evidence from Figure 2, indicating that the tests are affected by upward size distortions for small samples, which attenuate with increasing  $T$ . In this respect,  $\check{\tau}$  controls size best among the hypothesis tests across all scenarios, although it is somewhat conservative for  $\delta_A^*$ . Drastic improvements by scaling the regressors with adaptive weights are seen by comparing the spacing tests  $\mathcal{S}$  and  $\check{\mathcal{S}}$  with  $\mathcal{S}^{\text{LAR}}$ : even for large  $T$ , the plain spacing test  $\mathcal{S}^{\text{LAR}}$  remains too anti-conservative to be useful as a unit root test. We note that small sample size distortions are less pronounced across the adaptive variants and diminish quickly as  $T$  grows. This result not only confirms our theory on  $\tau$ , but further strengthens our conjecture in Remark 4 that  $\mathcal{S}$  and  $\check{\mathcal{S}}$  could have a correct size below  $\lambda_{\mathcal{O}}$  as  $T \rightarrow \infty$ . It seems likely that the spacing test can be tweaked for asymptotic validity in even more general settings than envisaged in Tibshirani et al. (2016, 2018), provided all coefficients are estimated consistently—a necessary condition for  $\tau$  and  $\check{\tau}$  as well.

For stationary data (bottom panel), we report size-adjusted power at 5% for  $\tau$ ,  $\check{\tau}$ ,  $\mathcal{S}$ , and  $\check{\mathcal{S}}$ , and present raw rejection rates for  $\mathcal{S}^{\text{LAR}}$ , since size-adjusted rates are mostly trivial given its empirical size. Columns for  $\text{AL}_{\text{BIC}}$  and  $\text{ALIE}_{\text{BIC}}$  show raw activation

Table 2: Empirical size and power of LARS solution path tests

	$T$	$\mathcal{S}^{\text{LAR}}$	$w_1 = 1/ \hat{\rho} , w_{2,j} = 1/ \hat{\delta}_j $			$\check{w}_1 =  J_\alpha/\hat{\rho} , w_{2,j} = 1/ \hat{\delta}_j $		
			$\tau$	$\mathcal{S}$	ALBIC	$\check{\tau}$	$\check{\mathcal{S}}$	ALIEBIC
$\rho^* = 0$								
$\delta_A^*$	50	.710	.256	.227	.224	.086	.157	.109
	75	.696	.166	.137	.140	.049	.094	.058
	100	.692	.129	.112	.103	.037	.079	.043
	150	.689	.100	.080	.070	.030	.064	.035
	250	.678	.075	.066	.051	.031	.059	.035
	500	.678	.068	.057	.042	.043	.060	.044
$\delta_B^*$	50	.154	.178	.137	.135	.118	.149	.127
	75	.111	.123	.090	.068	.090	.101	.079
	100	.105	.101	.079	.043	.072	.080	.055
	150	.097	.084	.073	.026	.072	.075	.044
	250	.097	.064	.053	.011	.054	.065	.021
	500	.096	.059	.058	.006	.052	.064	.014
$\delta_C^*$	50	.590	.174	.138	.100	.088	.142	.074
	75	.534	.125	.101	.049	.071	.098	.049
	100	.520	.094	.081	.032	.059	.088	.034
	150	.523	.086	.069	.019	.059	.070	.026
	250	.502	.066	.061	.010	.050	.067	.017
	500	.491	.059	.054	.003	.051	.061	.009
$\rho^* = -.05$								
$\delta_A^*$	50	.310	.002	.004	.394	.342	.113	.495
	75	.312	.041	.118	.540	.743	.277	.714
	100	.367	.309	.268	.672	.911	.405	.861
	150	.435	.857	.465	.872	.991	.548	.979
	250	.541	.997	.716	.988	1	.619	1
	500	.736	1	.900	1	1	.807	1
$\delta_B^*$	50	.216	.110	.096	.255	.151	.117	.311
	75	.254	.193	.156	.252	.251	.184	.355
	100	.294	.327	.197	.281	.419	.276	.432
	150	.414	.537	.308	.353	.634	.432	.571
	250	.557	.916	.652	.644	.955	.816	.855
	500	.669	.999	.956	.976	1	.985	.998
$\delta_C^*$	50	.652	.228	.255	.448	.544	.376	.604
	75	.808	.547	.443	.598	.814	.673	.810
	100	.907	.800	.643	.756	.950	.865	.925
	150	.971	.972	.886	.942	.995	.970	.994
	250	.995	1	.983	.999	1	.962	1
	500	1	1	1	1	1	.892	1

Notes: DGP (23).  $\delta_A^* = (.4, .3, .2, 0, 0, 0, -.2, 0, 0, .2)'$ ,  $\delta_B^* = (-.4, 0, .7)'$ ,  $\delta_C^* = .8$ . All methods are applied to model (3) with  $p = 10$  fixed.  $\mathcal{S}^{\text{LAR}}$ ,  $\mathcal{S}$ , and  $\check{\mathcal{S}}$  are LAR spacing tests for the irrelevance of  $y_{t-1}$  without adaptively weighted regressors, with all OLS weights and modified weights. ALBIC and ALIEBIC are BIC-tuned adaptive Lasso estimators.  $\tau$  and  $\check{\tau}$  are activation knot tests for the solution path to (5). The nominal level is 5%. Power is size-adjusted for all tests but  $\mathcal{S}^{\text{LAR}}$ . Adaptive Lasso solution paths are computed with  $\gamma_1 = \gamma_2 = 1$ . 5000 replications.

rates of  $y_{t-1}$ , as it is not possible to readily size adjust the true-positive rate of these consistent classifiers.<sup>4</sup> The non-adaptive  $\mathcal{S}^{\text{LAR}}$  is again found to be inferior to the competitors, as its raw power may be significantly below the size-adjusted power of the other methods. On the other hand,  $\mathcal{S}$  and  $\check{\mathcal{S}}$  have less size-adjusted power than  $\tau$  and  $\check{\tau}$ , despite the comparable size. As before, information enrichment proves to be beneficial in the sense that  $\check{\mathcal{S}}$  and  $\check{\tau}$  have higher power than their unmodified counterparts across all settings. Thus  $\check{\tau}$  is preferable to  $\tau$ , especially in scenario  $\delta_A^*$ , where  $\tau$  has low power for small  $T$ . Although a direct comparison is not feasible, the true positive rate of  $\text{ALIE}_{\text{BIC}}$  is roughly comparable to the power of  $\check{\tau}$  given similar empirical size, see setting  $\delta_B^*$  for  $T = 100$ . This observation indicates similar discriminatory power of decision rules based on consistent tuning or hypothesis testing. Further research here seems worthwhile but is beyond the scope of this paper.

## 4.2 Comparison to unit root tests in a near-integration framework

We next benchmark  $\tau$  and  $\check{\tau}$  against  $\text{MZ}_t$ ,  $\text{ADF}^{\text{GLS}}$  and  $J_\alpha$  in a near-integration setting where  $\varrho = 1+c/T$  with  $c \in (-\infty, 0]$ . The consistently tuned Lasso estimators are omitted as they do not have asymptotic power against alternatives in  $1/T$  neighbourhoods.

$\text{ADF}^{\text{GLS}}$  and the  $\text{MZ}_t$  are computed for GLS-adjusted data. Following the suggestions of Herwartz and Siedenburg (2010),  $J_\alpha$  is calculated with  $\alpha = .1$  and  $R = 150$ , after adjusting for deterministic components using OLS. Both  $J_\alpha$  and  $\text{MZ}_t$  require an estimate of the LRV  $\omega^2$ . Following Ng and Perron (2001) and Herwartz and Siedenburg (2010), we employ the autoregressive spectral density estimator at frequency zero,

$$\hat{\omega}_{\text{AR}}^2(k) := \frac{\hat{\sigma}_k^2}{(1 - \sum_{j=1}^k \hat{\delta}_j)^2}, \quad \hat{\sigma}_k^2 := (T - k)^{-1} \sum_{t=k+1}^T (\hat{e}_{k,t}^d)^2, \quad (24)$$

as proposed by Perron and Ng (1998). The  $\hat{e}_{k,t}^d$  are OLS residuals from the regression

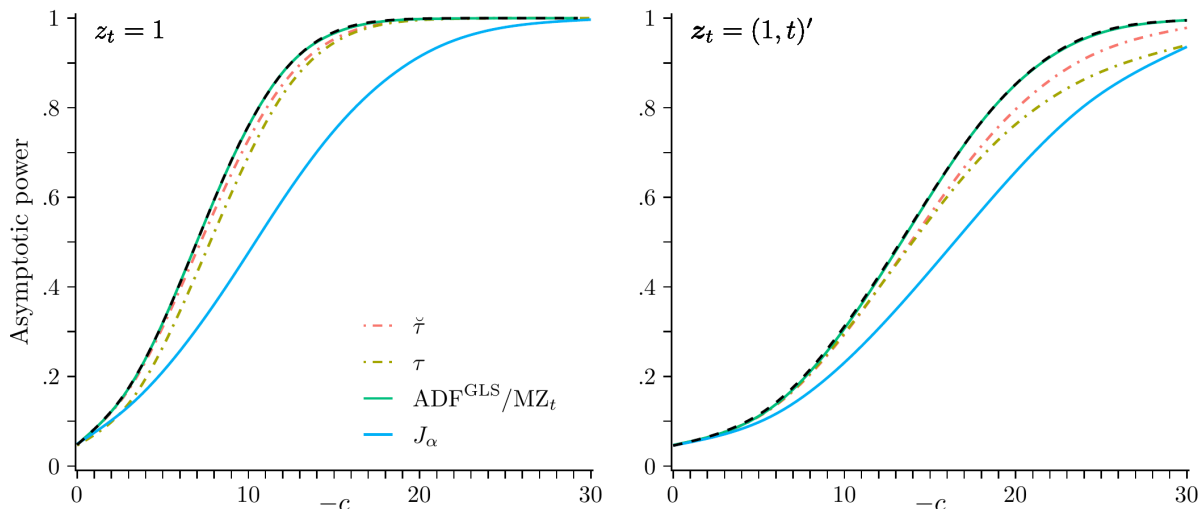
$$\Delta y_t^d = \xi_0 y_{t-1}^d + \sum_{j=1}^k \xi_j \Delta y_{t-j}^d + e_{k,t}^d, \quad (25)$$

based on the GLS-adjusted data  $y_t^d$  (if applicable). As suggested by Ng and Perron

---

<sup>4</sup>We consider detecting a stationary time series a *positive*.

Figure 3: Local asymptotic power functions of Lasso-based and classical unit root tests



Notes: 5% nominal level. The dashed black lines show the Gaussian asymptotic power envelopes of unit root tests for DGP (1) with a constant (left panel) and a linear time trend (right panel). Power functions of the tests are obtained by discrete approximations of  $W_c(r)$  with  $10^4$  steps and  $10^5$  replications.  $J_\alpha$  with  $\alpha = .1$  and  $R = 150$  is simulated for a Gaussian AR(1) DGP and used in approximating the power function of  $\check{\tau}$ .

(2001), we estimate  $k$  as  $\hat{k} := \arg \min_{0 \leq k \leq k_{\max}} \text{MAIC}(k)$  with

$$\text{MAIC}(k) := \log(\tilde{\sigma}_k^2) - 2 \frac{\tau_T(k) + k}{T - k_{\max}}, \quad (26)$$

the modified Akaike information criterion (AIC). The maximum lag order is  $k_{\max} = \lfloor 12(T/100)^{.25} \rfloor$  and  $\tilde{\sigma}_k^2 := (T - k_{\max})^{-1} \sum_{t=k+1}^T (\hat{e}_{k,t}^d)^2$  is a deviance estimate. The MAIC differs from the AIC by the stochastic adjustment term  $\tau_T(k) := (\tilde{\sigma}_k^2)^{-1} \hat{\xi}_0^2 \sum_{t=k_{\max}+1}^T (y_{t-1}^d)^2$  in the penalty function.  $\text{MZ}_t$  and  $\text{ADF}^{\text{GLS}}$  are implemented based on the regression (25) with  $k$  selected by MAIC. For  $\tau$  and  $\check{\tau}$ , we compute the Lasso solution paths to (4) with  $p = \hat{k}$  and consider FD-detrended data, cf. Section 3.5.

To analyse asymptotic efficiency, we compare the tests' asymptotic power in a Gaussian AR model with local-to-unity parameter  $c \in [0, -1, -2, \dots, -30]$  and zero initial condition. The asymptotic local power functions in Figure 3 obtain from  $10^5$  draws of discrete approximations of the corresponding limiting random variables with  $10^4$  steps. The dashed lines show the Gaussian asymptotic power envelope for unit root tests adjusting for the specified deterministic component. For a constant ( $z_t = 1$ , left panel) and a linear trend ( $z_t = (1, t)'$ , right panel), the asymptotic local power functions of  $\text{ADF}^{\text{GLS}}$  and  $\text{MZ}_t$  are virtually indistinguishable from the Gaussian power envelope by the construction of the tests.  $\tau$  and  $\check{\tau}$  track the power envelope, but show pronounced

downward deviations for  $\mathbf{z}_t = (1, t)'$  at smaller  $c$ . The results indicate that information enrichment is effective:  $\check{\tau}$  is often at least as powerful and outperforms  $\tau$  for  $z_t = 1$  and for processes with  $c < -15$  when  $\mathbf{z}_t = (1, t)'$ .

To investigate finite-sample powers in  $1/T$  neighbourhoods under correlated errors, we generate time series as

$$y_t = (1 + c/T)y_{t-1} + v_t, \quad t = -49, \dots, -1, 0, 1, \dots, T, \quad (27)$$

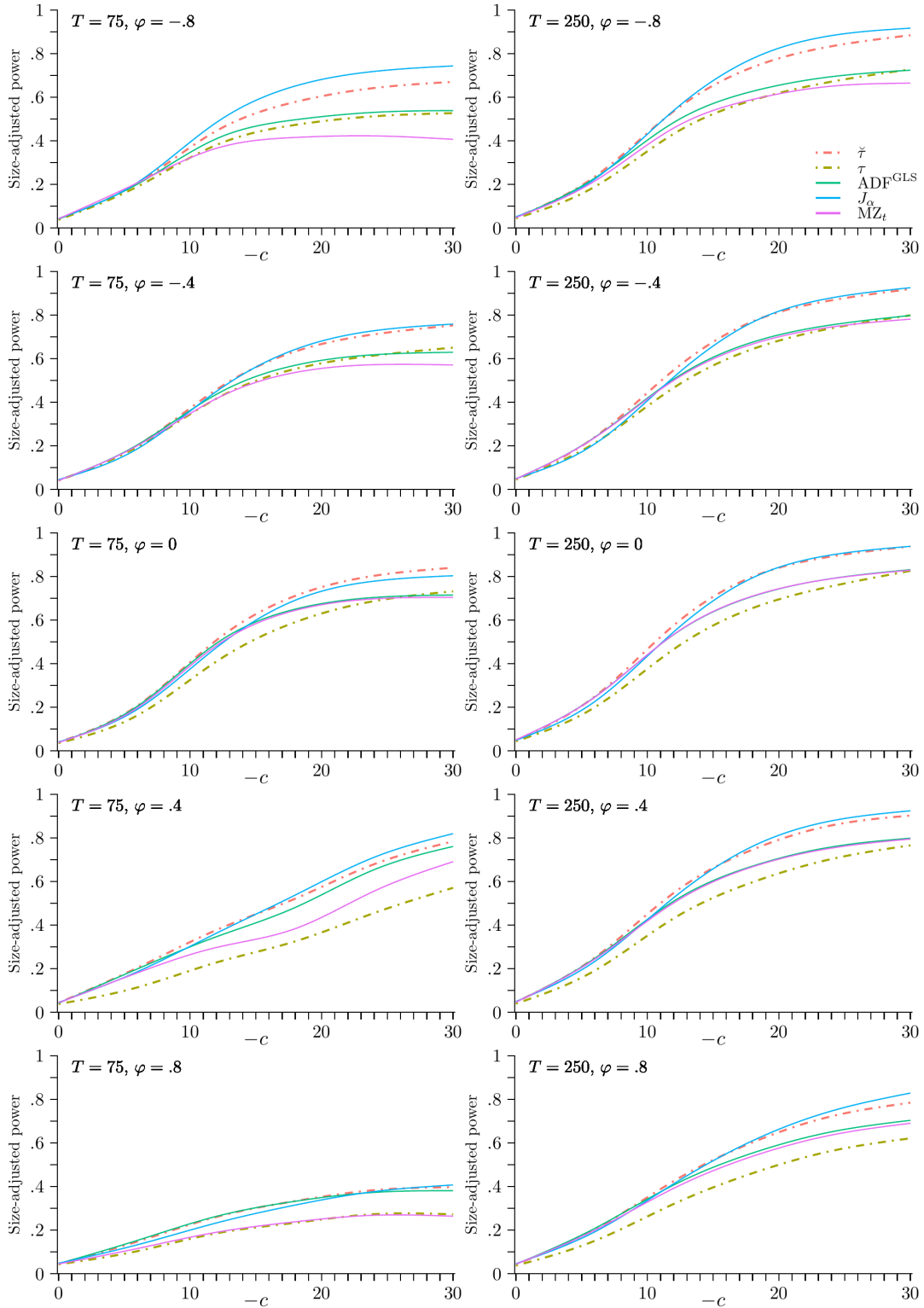
with starting value 0 and  $c \in [0, -1, -2, \dots, -30]$  for sample sizes  $T \in \{75, 250\}$ , discarding the first 50 samples. The errors  $v_t$  are generated by the ARMA recursion

$$v_t = \varphi v_{t-1} + \vartheta \epsilon_{t-1} + \epsilon_t, \quad \epsilon_t \stackrel{i.i.d.}{\sim} N(0, 1).$$

To model different degrees of persistence in the errors, we set  $\varphi, \vartheta \in \{-.8, -.4, 0, .4, .8\}$ , considering only pure AR and MA processes.

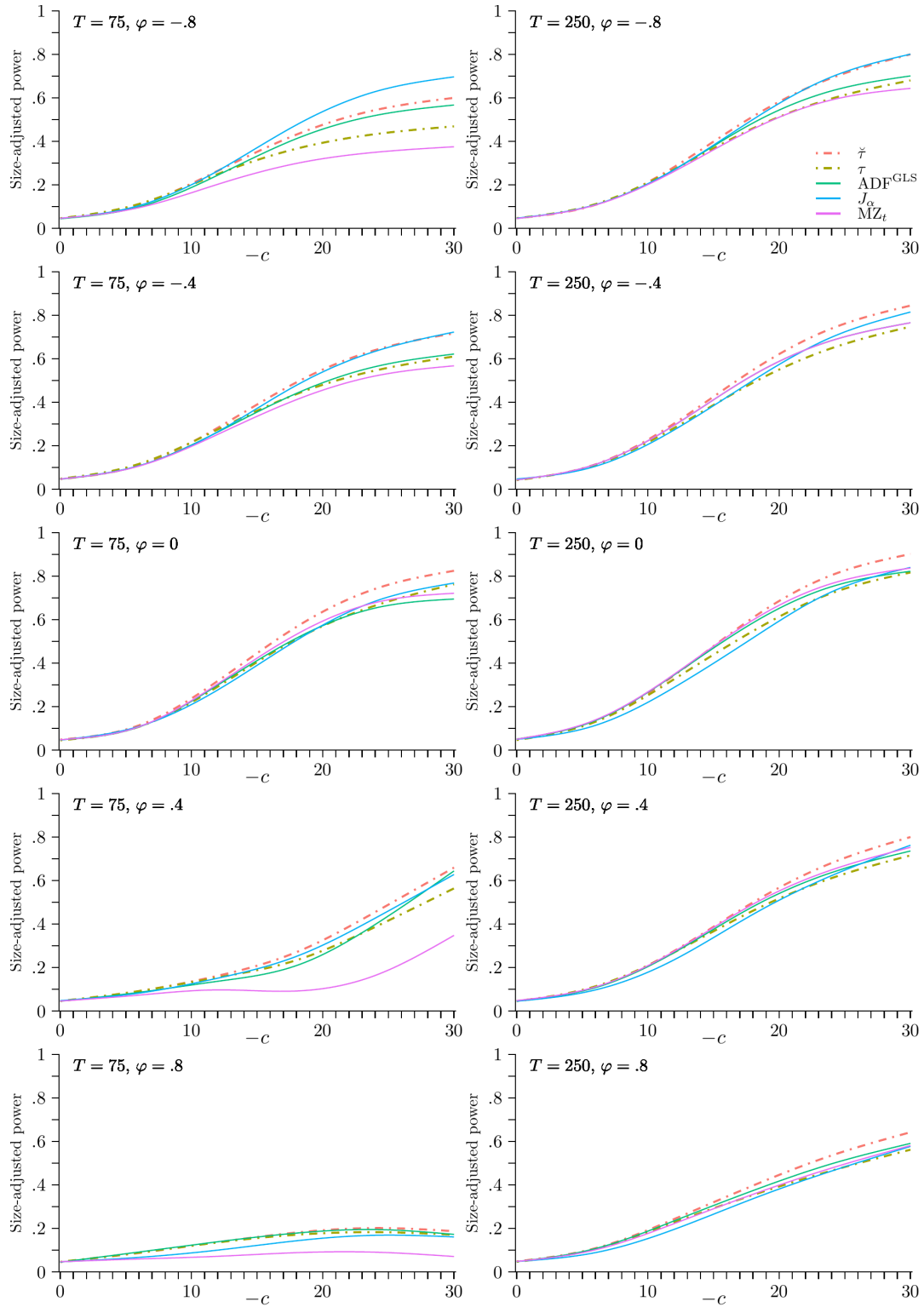


Figure 4: Size-adjusted local power – AR errors, constant



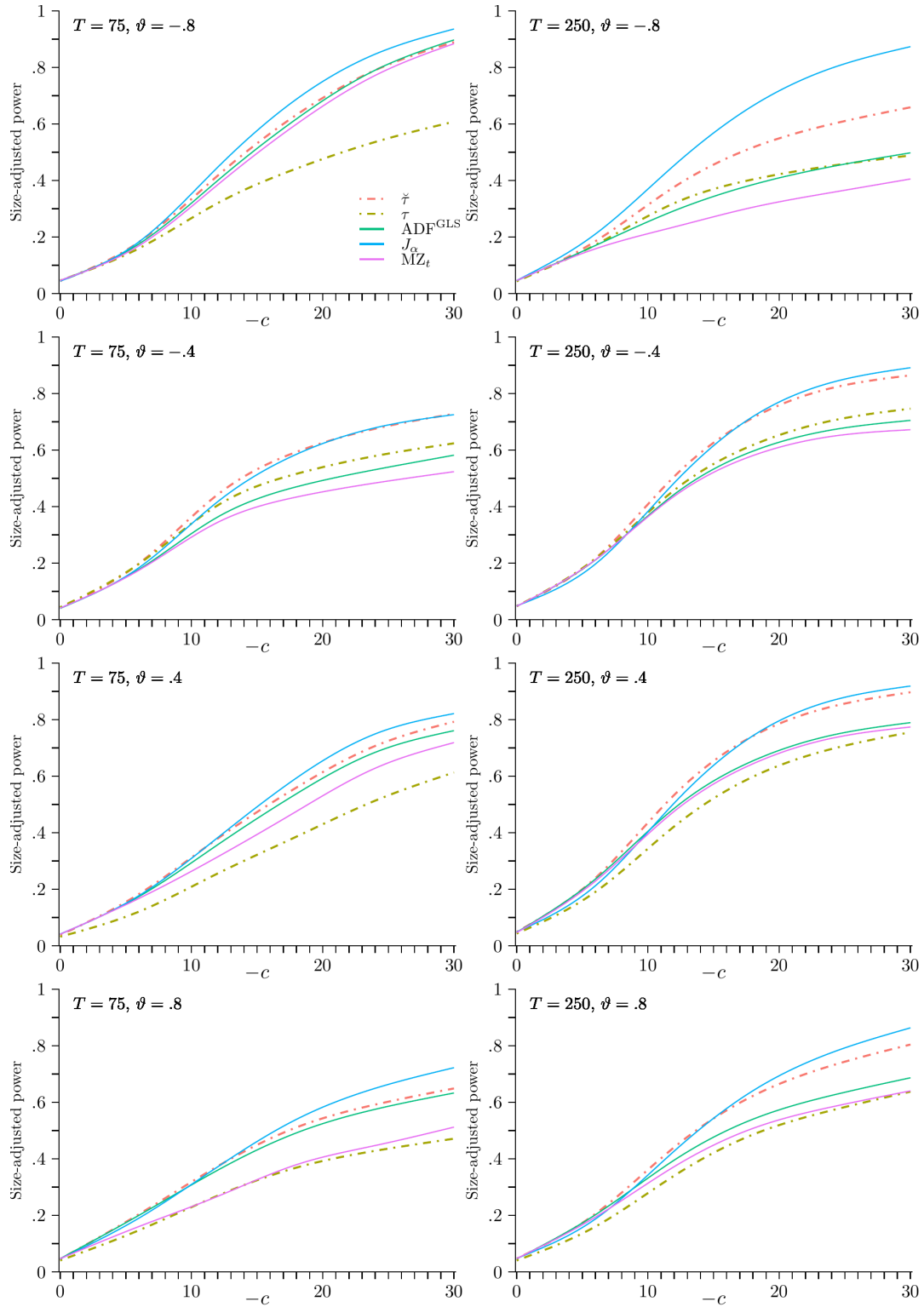
Notes: DGP (27) with  $\vartheta = 0$ . Model (3) with  $d_t = 0$ .  $\tau$  and  $\tilde{\tau}$  are activation knot tests based on FD-adjustment.  $\text{ADF}^{\text{GLS}}$  and  $\text{MZ}_t$  are GLS-adjusted ADF and Phillips-Perron tests.  $J_\alpha$  with  $\alpha = .1$  is computed for OLS-adjusted data. Lag orders are selected by MAIC with  $k_{\max} = \lfloor 12 \cdot (T/100)^{.25} \rfloor$ . Lines show 5<sup>th</sup>-degree natural cubic spline estimates of the size-adjusted local power functions at 5%. 5000 replications.

Figure 5: Size-adjusted local power – AR errors, linear time trend



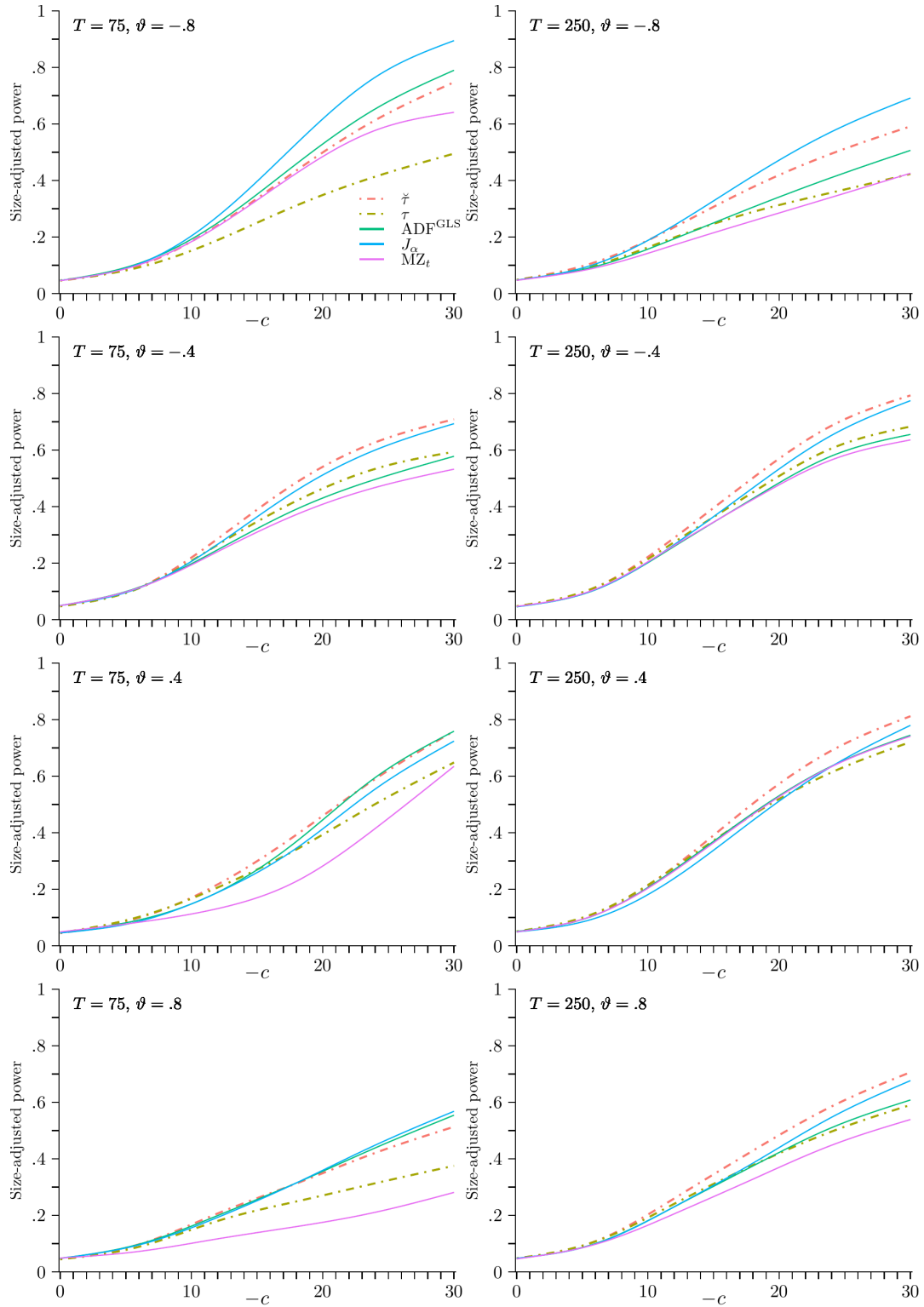
Notes: See Figure 4.

Figure 6: Size-adjusted local power – MA errors, constant



Notes: DGP (27),  $v_t = \vartheta\epsilon_{t-1} + \epsilon_t$ ,  $\epsilon_t \sim i.i.d. N(0,1)$ . See Figure 4 for details.

Figure 7: Size-adjusted local power – MA errors, linear time trend



Notes: See Figure 6.

Figures 4 and 5 show size-adjusted powers under AR errors for demeaned and detrended data. The results mirror the insight from the asymptotic local power function in Figure 3 that all tests have similar power for small  $c$ , which is lower under detrending and for highly correlated errors ( $\varphi = .8$ ). Depending on  $\varphi$ , we find substantial discrepancies for larger  $c$ . These are most pronounced at  $\varphi = -.8$ , where  $J_\alpha$  performs best. Overall,  $\check{\tau}$  tracks  $J_\alpha$ , dominating  $\tau$  due to the enrichment via  $\check{w}_1$ . While there is no clear ranking across  $c$  and  $\varphi$ , the size-adjusted power of  $\check{\tau}$  is often significantly higher than for  $\text{ADF}^{\text{GLS}}$  and  $\text{MZ}_t$ .

We report similar results for MA errors in Figures 6 and 7. Striking deviations between the tests arise for detrending under large negative MA coefficients at  $T = 75$ , which is one of the few scenarios where  $\text{ADF}^{\text{GLS}}$  surpasses  $\check{\tau}$ . It is, however, well-known that unit root tests suffer from upward size distortions in these scenarios (cf. Ng and Perron, 2001), making it difficult to recommend one test over the others. We examine this point below.

To investigate the dependence on the sample size, we further generate data using (27) for fixed  $\rho^*$  and  $T \in \{50, 75, 100, 150, 250, 500\}$  and again test at 5%. We set  $c = 0$  to generate non-stationary data. Tables D3 and D4 in Appendix D present the empirical sizes of the tests for AR errors. The activation knot tests are close to the nominal level across parameter combinations and can compete with established unit root tests. Negative  $\varphi$  are exemptions where  $\tau$  and  $\check{\tau}$  are slightly oversized. This behaviour is more pronounced under detrending but vanishes quickly with  $T$ .

We set  $c = -7$  and  $c = -13.5$  as local alternatives in the constant and in the trend-adjusted case, respectively. Size-adjusted powers for AR errors are presented in the Tables D6 and D7 in Appendix D. The results confirm that  $\check{\tau}$  has higher rejection rates than the  $\tau$  test for all  $\varphi$  considered and across  $T$ . This observation further corroborates our conjecture that power enhancements of the consistently tuned adaptive Lasso from the modified penalty weight  $\check{w}_1$  reported in Arnold and Reinschlüssel (2023) carry over to  $\check{\tau}$ . Another indication of this feature is that the  $\check{\tau}$  test often exceeds the power of  $J_\alpha$ , as indicated by the asymptotic results in Figure 3.  $\check{\tau}$  hence comes closer to the theoretical upper bound of 50% local asymptotic power achievable by an optimal unit root test for the alternatives with  $c = -7$  and  $c = -13.5$ . Power gains not vanishing for samples of size  $T = 1000$  substantiate this result. In this respect,  $\check{\tau}$  benchmarks comparably to the  $\text{ADF}^{\text{GLS}}$  test and sometimes even outperforms it.

Similar outcomes are obtained in case of MA errors for which we report empirical sizes in Tables D9 and D10 and size-adjusted powers in Tables D12 and D13 in Appendix D.

Noteworthy here is a weak spot of the activation knots test for negative MA coefficients under the null. All tests suffer from significant upward size distortions in such scenarios. However, the type I error rates for the activation knot tests are higher than for the other tests and need larger  $T$  to diminish. This effect is strongly pronounced for detrending, although  $\tilde{\tau}$  does better than  $\tau$ . Research on the causes of this phenomenon is certainly of interest.

## 5 Application to German groundwater levels

At present, over seventy per cent of Germany’s water demand for irrigation and drinking water production is met by groundwater reserves, which often are the sole regional source of water supply, particularly in the northeastern federal states (Umweltbundesamt, 2018). Climate change and anthropogenic influences are suspected to exert a negative impact on regional groundwater supplies in recent decades. Deep learning forecasts across possible climate pathways indicate further substantial declines until the end of the century for the whole country, see Wünsch et al. (2022).

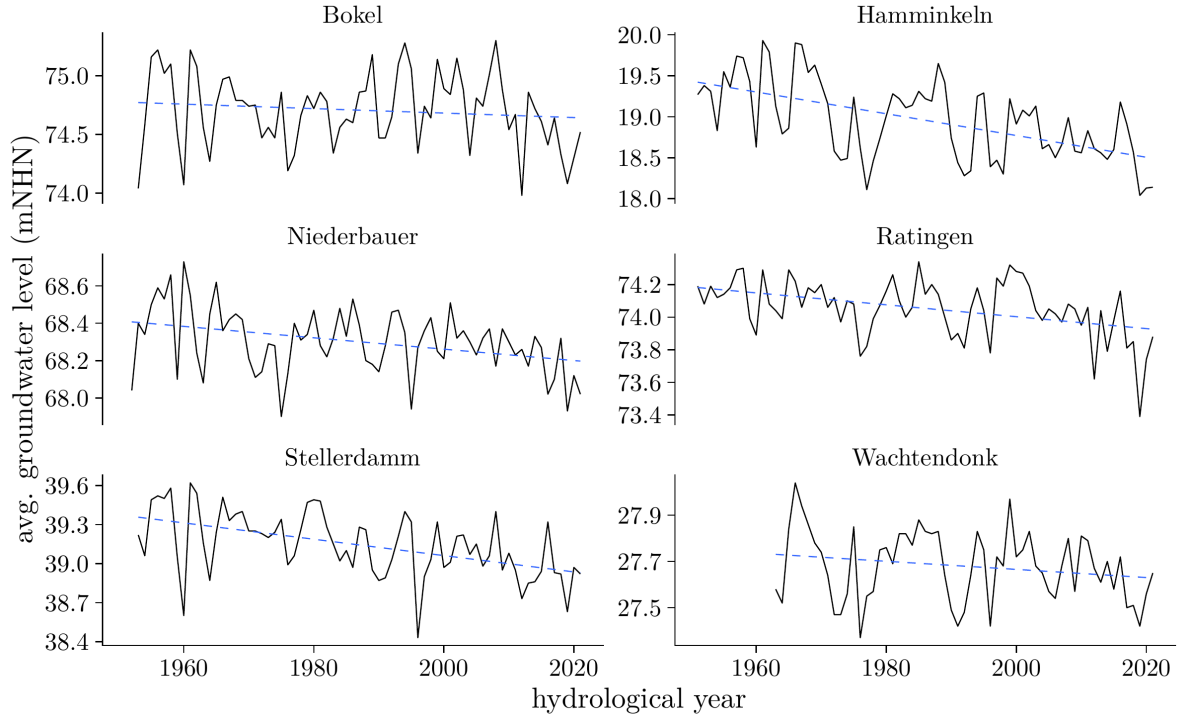
Reductions in groundwater levels may result in several economic ramifications, including increased expenditures for municipal drinking water supply, agricultural production drops and profitability declines due to elevated costs for irrigation, and the prospect of production disruptions within the industrial sector, to name a few (Wünsch et al., 2022). Managing water resources will hence pose challenges for German policymakers. In particular, it is essential to enact countermeasures early to mitigate the risk of shortages caused by seasonal demand peaks during prolonged dry periods in the following decades, cf. Scheihing et al. (2022).

### 5.1 Data and models

For the empirical analysis, we examine six groundwater level time series recorded at official monitoring stations in the federal state of North Rhine-Westphalia (NRW). We consider stations for which particularly long samples are available, with low anthropogenic influence. These stations are located in the municipalities of Bokel (city of Rietberg), Hamminkeln, Niederbauer, Ratingen, Stellerdamm (city of Rahden) and Wachtendonk. Positions within Germany are shown in Figure C1.

We use the average groundwater level of the hydrological year, measured as the height above sea level in meters (mNHN), as the indicator. The data are freely available from

Figure 8: Evolution of groundwater levels in NRW, Germany



*Notes:* A hydrological year is from November 1 to October 31. Levels are the height above sea level in meters (mNHN), measured as the difference in elevation between the measuring point in the German elevation reference system and the groundwater level. Dashed lines show linear trend estimates.

the NRW State Office for Nature, Environmental and Consumer Protection (LANUV, 2023). The evolution of groundwater levels and estimated linear trends are shown in Figure 8. This preliminary analysis indicates downward trends in all regions.

We apply the procedures to data adjusted for a constant or a constant and a linear time trend. Regarding the DGP (1), these appear reasonable specifications: In the case of a constant  $\theta_1$ , we test the null of groundwater levels following a purely stochastic trend against a stationary process with a non-zero mean. When adjusting for a linear trend component  $\mathbf{z}_t = (1, t)'$  with coefficients  $\boldsymbol{\theta} = (\theta_1, \theta_2)'$ , we test the null of a random walk (possibly with drift) against stationary fluctuations around a deterministic time trend.

Given the low power of univariate procedures in small samples, a panel unit root test would be appropriate for a thorough analysis. However, the example serves to illustrate the differences between the methods in empirical applications.

## 5.2 Empirical results

Table 3 presents the results. In addition to the five tests considered, we also report the classification result obtained from the BIC-tuned adaptive Lasso estimators with all-OLS weights in column  $\tau$  and weight  $\check{w}_1 = (\hat{\rho}/J_\alpha)^{-1}$  in column  $\check{\tau}$ . Grey shading indicates classification as stationary. Evidence for a stationary process (top panel) is inconclusive. None of the methods rejects the null hypothesis at common significance levels for the sites Bokel, Ratingen, and Stellerdamm. Evidence is mixed for Hamminkeln and Niederbauer. For the former, only  $\check{\tau}$  rejects at 5% among the hypothesis tests. For Niederbauer, the activation knot tests and  $\text{ADF}^{\text{GLS}}$  are significant, whereby marginal significance levels (in parentheses) range from three to nine per cent. The tuned adaptive Lasso estimators classify water levels at Niederbauer and Hamminkeln as stationary. An exception is Wachtendonk, where all procedures reject the null of a random walk.

Evidence favouring trend-stationary processes (bottom panel) is substantial across measuring sites. All tests reject the null of a stochastic trend in groundwater levels at significance levels below 1% for the sites Hamminkeln, Ratingen, Stellerdamm and Wachtendonk. For Niederbauer,  $J_\alpha$  is the only hypothesis test with a significant outcome at 5%. The tuned adaptive Lasso estimators classify measurements at Niederbauer as trend-stationary, whereas the corresponding activation knot tests do not. As for the case with a constant, none of the procedures indicate a (trend-)stationary process for Bokel. Overall, these results substantiate the conjecture that groundwater levels are stationary around a deterministic trend rather than following a stochastic trend.

The empirical results mirror the Monte Carlo results, which show that the activation knot tests track the established unit root tests, often yielding similar results. We further find that information enrichment can be helpful in empirical applications:  $\check{\tau}$  rejects the null hypothesis of a random walk the most often among the hypothesis tests. In the case with a constant,  $J_\alpha$  has the second lowest p-value for Hamminkeln, and its impact via the adaptive penalty weight leads to a rejection based on  $\check{\tau}$  at 10% while  $\tau$  has p-value 16%. In the linear trend case for Niederbauer, a comparison with  $\tau$  shows that  $\check{\tau}$  is pushed markedly towards the margin of rejection by the adaptive weight.



Table 3: Inference on stochastic trends in German groundwater level time series

location	$T$	$\tau$	$\check{\tau}$	ADF <sup>GLS</sup>	MZ <sub><math>t</math></sub>	$J_\alpha$
$z_t = 1$ ( <i>constant</i> )						
Bokel (1953–2021)	69	0.90 (.40)	.79 (.33)	−0.94 (.48)	−0.38 (.69)	1.10 (.31)
Hamminkeln (1951–2021)	71	2.23 (.16)	3.17* (.10)	−1.44 (.23)	−1.26 (.27)	.81 (.14)
Niederbauer (1952–2021)	80	5.00** (.03)	4.83* (.06)	−1.94* (.09)	−.65 (.58)	1.03 (.25)
Ratingen (1951–2021)	71	.01 (.93)	.01 (.90)	−.81 (.54)	−1.01 (.40)	.89 (.18)
Stellerdamm (1953–2021)	69	.08 (.82)	.04 (.83)	−.56 (.66)	−.40 (.68)	1.68 (.59)
Wachtendonk (1963–2021)	59	11.91*** ( $<1e-6$ )	45.48*** ( $3e-4$ )	−3.56*** ( $<1e-6$ )	−3.07*** ( $1e-4$ )	.26*** ( $3e-4$ )
$z_t = (1, t)'$ ( <i>linear time trend</i> )						
Bokel (1953–2021)	69	2.60 (.39)	1.70 (.53)	−0.86 (.95)	−0.49 (.98)	1.40 (.70)
Hamminkeln (1951–2021)	71	16.95*** ( $6.9e-4$ )	61.47*** ( $1.6e-4$ )	−5.10*** ( $9.4e-5$ )	−3.66*** ( $1.8e-4$ )	.28*** ( $1.6e-4$ )
Niederbauer (1952–2021)	80	2.40 (.44)	6.53 (.13)	−2.08 (.37)	−1.60 (.59)	.50** (.02)
Ratingen (1951–2021)	71	31.69*** ( $8e-6$ )	87.28*** ( $3.6e-5$ )	−4.46*** ( $8.3e-4$ )	−3.65*** ( $1.9e-4$ )	0.36*** (.0020)
Stellerdamm (1953–2021)	69	37.57*** ( $<1e-6$ )	208.72*** ( $<1e-6$ )	−6.64*** ( $<1e-6$ )	−3.97*** ( $2e-6$ )	.18*** ( $<1e-6$ )
Wachtendonk (1963–2021)	59	14.60*** ( $<1e-6$ )	40.95*** ( $8.1e-4$ )	−3.85*** (.01)	−3.25*** ( $1.8e-4$ )	.36*** ( $8.1e-4$ )

Notes: Data are adjusted for the stated deterministic component. AL estimators in columns  $\tau$  and  $\check{\tau}$  are computed using the FD approach in Schmidt and Phillips (1992). Grey shading indicates classification as stationary by the corresponding BIC-tuned AL estimator. Values in parenthesis are marginal significance levels obtained from simulation. For MZ <sub>$t$</sub>  and  $J_\alpha$  the LRV is estimated by  $\hat{\omega}_{AR}^2$ . All lag orders are computed by MAIC with maximum lag order  $p = \lfloor 12 \cdot (100/T)^{.25} \rfloor$ .

## 6 Conclusion and outlook

Conventional methods for inference based on the (adaptive) Lasso and its solution path require tuning, sophisticated post-selection procedures or conditioning on random hypotheses. Tuning-based methods, in particular, may suffer from uncontrolled classification error rates or a lack of power against local alternatives.

Focusing on the potentially non-stationary regressor  $y_{t-1}$  in ADF regressions, we studied the distribution of its activation knot  $\lambda_{0,\rho^*}$  on the adaptive Lasso’s solution path and used an appropriate scaling to devise a significance test for the relevance of  $y_{t-1}$ . The

novel test  $\tau_{\gamma_1}$  exploits that the oracle property of the adaptive Lasso implies different stochastic orders of  $\lambda_{0,\rho^*}$  for stationary and non-stationary data. Our proposed implementation  $\tau$  follows naturally from the output of the algorithm (Efron et al., 2004) as implemented in the R package `lars` (Hastie & Efron, 2022) and is straightforward to compute.

The new test is compared with testing in the post-selection framework of Lee et al. (2016) and Tibshirani et al. (2016) where inference is conditional on  $\widehat{\mathcal{M}}$  which is subject to the stochastic variable selection process. We contrast  $\tau$  in detail with the spacing test of Tibshirani et al. (2016), which tests whether the partial regression coefficient of  $y_{t-1}$  at its LAR activation knot is zero, conditional on the lagged dependent variables that are currently in the model. Instead,  $\tau$  performs inference based on the asymptotic null distribution of  $\lambda_{0,\rho^*=0}$ , which is tractable if the adaptive Lasso can consistently estimate the coefficients.

Noting that the  $\tau$  test is significantly influenced by the adaptive penalty weight of  $y_{t-1}$  in the adaptive Lasso loss function, we propose a modified version of the new test, using the enhanced weight  $\check{w}_1$ . This modified test  $\check{\tau}$  is based on the information-enrichment principle considered in Arnold and Reinschlüssel (2023) for improving the classification performance of tuned adaptive Lasso estimators in ADF models. In addition to the OLS coefficient estimate of  $y_{t-1}$ ,  $\check{\tau}$  incorporates a second identification principle regarding the relevance of the regressor to compute the penalty weight. Analogously to the construction of the ALIE estimator proposed by Arnold and Reinschlüssel (2023), we make use of the  $J_\alpha$  statistic of Herwartz and Siedenburg (2010) which exploits distinct orders in probability of the OLS estimator in time series regressions where the degree of integration differs.

Our Monte Carlo comparison of LARS-computed tests shows that  $\tau$  and  $\check{\tau}$  are significantly more reliable than the spacing test for LAR, which is often heavily oversized and has considerably lower power. We also found power shortfalls but mitigated size distortions for two suggested adaptive LAR spacing tests. Information enrichment with  $\check{w}_1$  curbs size distortions and yields a higher size-adjusted power for the spacing test and  $\check{\tau}$ , which performs best. These results suggest that performance gains through information enrichment do not confine to tuning-based inference (cf. Arnold and Reinschlüssel, 2023) but extend well to hypothesis testing. While  $\tau$  and  $\check{\tau}$  have similar precision under the null, we showed that  $\check{\tau}$  is superior to  $\tau$  in a local power analysis. Both methods keep up with or outperform established unit root tests under local alternatives in  $1/T$  neighbourhoods for ARMA DGPs. A weak spot of the new tests is large negative MA

coefficients, which entail slowly vanishing upward size distortions that are pronounced under detrending—a feature that also affects established unit root tests.

Applying the tests to German groundwater levels, we found evidence of declines along deterministic trends over the last seven decades for five out of six monitoring sites. The outcomes mostly agree with results from other unit root tests and consistently tuned adaptive Lasso estimators. However, we find differences in outcomes that reflect some of the observed characteristics in the Monte Carlo simulations, pointing to the benefits of information enrichment.

There are several directions for further research. First, augmenting the ADF regression with other (exogenous) covariates similar to ARX regressions could improve power for stationary data with a low signal-to-noise ratio. Assuming the coefficients of additional covariates can be consistently estimated, this would be a straightforward extension, not incurring any nuisance parameters. An extension of the test to saturated models with  $p \geq T$  seems also worth investigating. The central issue is that we require consistent coefficient estimates for all covariates, including those erroneously activated. A path forward may follow the post-double-selection procedure (Belloni et al., 2013). Such an approach would enable practitioners to apply our test to high-dimensional regressions where the number of (potential) covariates grows faster than our assumptions allow.

Furthermore, using  $\tau$  instead of cross-validation or the AIC to select  $\lambda$  could aid the detection of small effects or raise power against local alternatives in post-selection inference. A significant advantage of using  $\tau$  rather than tuning is reliable control of the classification error rate in conservative model selection. Comparing the performance of popular conservative tuning criteria with  $\tau$  would be an interesting exercise easy to implement within the framework of stationary time series regressions since all  $\lambda_0, \delta_j^*=0$ -distributions are identical. Using  $\tau$  to tune cross-section regressions is just as appealing, but requires knowledge about all  $\lambda_0, \beta_j^*=0$ -distributions, which may vary across the covariates.

Finally, it would be interesting to investigate whether our test principle transfers to cross-section regression, e.g., for causal analysis. Similar to the bootstrap for the spacing test presented in Tibshirani et al. (2018), advances in the bootstrap literature summarised in Chernozhukov et al. (2023) could help recover the null distribution in such scenarios, possibly even in high-dimensional regressions. A multiplier (or wild) bootstrap could also be useful to improve the precision of the tests under detrending with MA errors and provide robustness to non-stationary volatility. We are currently investigating this the idea.

## A Proofs

### *Proof of Theorem 1.*

1. We divide the proof to result 1 of Theorem 1 into three parts. In part (a), we show that the adaptive Lasso estimator  $\hat{\beta}_\lambda$  for sequences  $\lambda$  in the interval  $[0, \lambda_{\mathcal{O}}]$  is consistent for  $\beta_0^*$ , the *fixed* limit of  $\beta^*$  as  $T \rightarrow \infty$  under Assumptions 1 and 2. The notion of  $\beta_0^*$  allows  $\beta^*$  to depend on  $T$  to cover local-to-unity processes. Because  $\lambda_{0, \rho^* \sim c/T} \in [0, \lambda_{\mathcal{O}}]$ ,  $\hat{\beta}_\lambda$  must be consistent for any  $\lambda = \lambda_{0, \rho^* \sim c/T}$  with  $c \in (-\infty, 0]$ . Part (b) uses this property and analyses the asymptotic behaviour of  $\lambda_{0, \rho^* \sim c/T}$ , appealing to results from Aylar et al. (2019) who generalise the asymptotic theory for OLS estimators of model (3) under lag truncation introduced by Chang and Park (2002) to processes with local alternatives. The limits derived in part (b) allow us to identify the limit distribution of  $\tau_{\gamma_1}$ , which is summarised in part (c).

(a) We begin by proving the consistency of  $\hat{\beta}_\lambda$  in model (3) under Assumptions 1 and 2 if the penalty parameter  $\lambda$  satisfies  $\lambda = O(\lambda_{\mathcal{O}})$ . Denote  $\mathbf{X}$  the  $(T - p - 1) \times (p + 1)$  design matrix of model (3) and consider the partition  $\mathbf{X} = (\mathbf{X}_{\mathcal{M}} : \mathbf{X}_{-\mathcal{M}})$  with the sub-matrix  $\mathbf{X}_{\mathcal{M}}$  containing the relevant regressors  $\mathbf{x}_i \in \mathcal{M}$  and  $\mathbf{X}_{-\mathcal{M}}$  the irrelevant ones. The DGP coefficient vector  $\beta^* = (\beta_{\mathcal{M}}', \beta_{-\mathcal{M}}')' = (\beta_{\mathcal{M}}', \mathbf{0}')'$  is partitioned analogously. We rewrite the adaptive Lasso loss function (5) accordingly as

$$\begin{aligned} \Psi_T(\dot{\beta}_{\mathcal{M}}, \dot{\beta}_{-\mathcal{M}}|\lambda) &= \left\| \Delta \mathbf{y} - \mathbf{X}_{\mathcal{M}} \dot{\beta}_{\mathcal{M}} - \mathbf{X}_{-\mathcal{M}} \dot{\beta}_{-\mathcal{M}} \right\|_2^2 \\ &\quad + 2\lambda \left\| \mathbf{w}_{\mathcal{M}} \odot \dot{\beta}_{\mathcal{M}} \right\|_1 + 2\lambda \left\| \mathbf{w}_{-\mathcal{M}} \odot \dot{\beta}_{-\mathcal{M}} \right\|_1, \end{aligned} \quad (\text{A28})$$

where  $\mathbf{w}_{\mathcal{M}}$  and  $\mathbf{w}_{-\mathcal{M}}$  denote the stacked penalty weights for some  $\gamma_1 > 1/2, \gamma_2 > 0$ . After rescaling with  $1/T$ , we obtain the limit loss function

$$\begin{aligned} \Psi_0(\dot{\beta}_{\mathcal{M}}, \dot{\beta}_{-\mathcal{M}}|\lambda) &:= \lim_{T \rightarrow \infty} \frac{1}{T} \Psi_T(\dot{\beta}_{\mathcal{M}}, \dot{\beta}_{-\mathcal{M}}|\lambda) \\ &= \lim_{T \rightarrow \infty} \frac{1}{T} \left\| \Delta \mathbf{y} - \mathbf{X}_{\mathcal{M}} \dot{\beta}_{\mathcal{M}} - \mathbf{X}_{-\mathcal{M}} \dot{\beta}_{-\mathcal{M}} \right\|_2^2 \\ &\quad + \lim_{T \rightarrow \infty} \frac{2\lambda}{T} \left\| \mathbf{w}_{\mathcal{M}} \odot \dot{\beta}_{\mathcal{M}} \right\|_1 + \lim_{T \rightarrow \infty} \frac{2\lambda}{T} \left\| \mathbf{w}_{-\mathcal{M}} \odot \dot{\beta}_{-\mathcal{M}} \right\|_1. \end{aligned} \quad (\text{A29})$$

Define  $\mathcal{B}$  as the set of all solutions along the Lasso path for  $\lambda \in [0, \infty)$ ,

$$\mathcal{B} := \bigcup_{\lambda \in [0, \infty)} \left\{ (\hat{\beta}'_{\lambda, \mathcal{M}}, \hat{\beta}'_{\lambda, -\mathcal{M}})' := \arg \min_{\dot{\beta}_{\mathcal{M}}, \dot{\beta}_{-\mathcal{M}}} \Psi_0(\dot{\beta}_{\mathcal{M}}, \dot{\beta}_{-\mathcal{M}}|\lambda) \right\}.$$

Because  $\mathcal{B}$  exclusively contains minimisers which by definition improve on the path's starting point  $\Psi_0(\mathbf{0}, \mathbf{0}|\lambda)$  for  $\lambda \geq \max_i \lambda_{0, \beta_i \neq 0}$ , the limit loss function  $\Psi_0(\dot{\beta}_{\mathcal{M}}, \dot{\beta}_{-\mathcal{M}}|\lambda)$  is bounded for every element in  $\mathcal{B}$ , we have

$$\begin{aligned} (\dot{\beta}'_{\mathcal{M}}, \dot{\beta}'_{-\mathcal{M}})' \in \mathcal{B}: \quad \Psi_0(\dot{\beta}_{\mathcal{M}}, \dot{\beta}_{-\mathcal{M}}|\lambda) &\leq \Psi_0(\mathbf{0}, \mathbf{0}|\lambda) \\ &= \text{E}(\Delta y_t^2) \\ &< \infty, \end{aligned}$$

where existence of  $\text{E}(\Delta y_t^2)$  is ensured by weak stationarity. Therefore, the limit loss function exists for *all* solutions on the Lasso path.<sup>5</sup>

Supposing that  $\lambda = O(\lambda_{\mathcal{O}})$  and  $\dot{\beta}_{\mathcal{M}} \in \mathcal{B}$  hereafter,

$$\text{plim} \frac{2\lambda}{T} \|\mathbf{w}_{\mathcal{M}} \odot \dot{\beta}_{\mathcal{M}}\|_1 = \mathbf{0}, \quad (\text{A30})$$

since all elements of  $\mathbf{w}_{\mathcal{M}}$  are  $O_p(T^{-1/2})$ ,  $\lambda_{\mathcal{O}} = o(T^{1/2})$  by construction and the dimension of each  $\mathbf{w}_{\mathcal{M}}$  and  $\beta_{\mathcal{M}}$  is bounded by  $p = o(T^{1/3})$ .

The limit of the second  $\ell_1$ -penalty term in (A29) has a lower bound attained at  $\beta_{0, -\mathcal{M}}^* = \mathbf{0}$ ,

$$\lim_{T \rightarrow \infty} \frac{2\lambda}{T} \|\mathbf{w}_{-\mathcal{M}} \odot \dot{\beta}_{-\mathcal{M}}\|_1 \begin{cases} = 0, & \text{if } \dot{\beta}_{-\mathcal{M}} = \mathbf{0} \\ \in [0, \infty), & \text{if } \dot{\beta}_{-\mathcal{M}} \neq \mathbf{0} \end{cases}, \quad (\text{A31})$$

with the second case's value depending on the choices for  $\gamma_1, \gamma_2$  and the growth rate of  $\lambda$ .

Recalling that collinearity is ruled out since Assumption 2 ensures  $\mathbf{X}$  to have full column rank, results (A30) and (A31) establish a lower limit for  $\Psi_0(\cdot, \cdot|\lambda)$ ,

$$\inf_{\dot{\beta}_{\mathcal{M}}, \dot{\beta}_{-\mathcal{M}}} \Psi_0(\dot{\beta}_{\mathcal{M}}, \dot{\beta}_{-\mathcal{M}}|\lambda) = \Psi_0(\beta_{0, \mathcal{M}}^*, \mathbf{0}|\lambda) = \sigma^2. \quad (\text{A32})$$

Because  $\beta_0^* := (\beta_{0, \mathcal{M}}^*, \mathbf{0})'$  uniquely minimises the quadratic component of the loss function (A29) and attains the zero infima of the terms in (A30) and (A31),

---

<sup>5</sup>Note that this property also holds for the finite-sample loss function  $\Psi_T$  but omit the argument for brevity.

it must be the unique minimiser of  $\Psi_0(\cdot, \cdot | \lambda)$ :

$$\begin{aligned} \Psi_0(\dot{\beta}_{\mathcal{M}}, \dot{\beta}_{-\mathcal{M}} | \lambda) - \Psi_0(\beta_{0, \mathcal{M}}^*, \mathbf{0} | \lambda) &> 0 \quad \forall (\dot{\beta}'_{\mathcal{M}}, \dot{\beta}'_{-\mathcal{M}})' \neq (\beta_{0, \mathcal{M}}^*, \mathbf{0})', \\ \Psi_0(\dot{\beta}_{\mathcal{M}}, \dot{\beta}_{-\mathcal{M}} | \lambda) - \Psi_0(\beta_{0, \mathcal{M}}^*, \mathbf{0} | \lambda) &= 0 \quad \text{iff } (\dot{\beta}'_{\mathcal{M}}, \dot{\beta}'_{-\mathcal{M}})' = (\beta_{0, \mathcal{M}}^*, \mathbf{0})'. \end{aligned}$$

Therefore  $\beta_0^*$ , the fixed limit of  $\beta^*$  as  $T \rightarrow \infty$  is *identified* in  $\Psi_0(\dot{\beta}_{\mathcal{M}}, \dot{\beta}_{-\mathcal{M}} | \lambda)$  for  $\lambda = O(\lambda_{\mathcal{O}})$ . As  $T \rightarrow \infty$ , the minimum of the sample loss function (A28) (epi-)converges to the limit loss function's unique minimum,

$$\begin{aligned} \frac{1}{T} \Psi_T(\beta_{0, \mathcal{M}}^*, \mathbf{0} | \lambda) &= \frac{1}{T} \|\Delta \mathbf{y} - \mathbf{X}_{\mathcal{M}} \beta_{0, \mathcal{M}}^*\|_2^2 + \frac{2\lambda}{T} \|\mathbf{w}_{\mathcal{M}} \odot \beta_{0, \mathcal{M}}^*\|_1 \\ &\xrightarrow{p} \sigma^2 + o_p(1) \\ &= \min_{\dot{\beta}_{\mathcal{M}}, \dot{\beta}_{-\mathcal{M}}} \Psi_0(\dot{\beta}_{\mathcal{M}}, \dot{\beta}_{-\mathcal{M}} | \lambda) \quad \forall \lambda = O(\lambda_{\mathcal{O}}). \end{aligned}$$

Hence the adaptive Lasso estimator  $\hat{\beta}_{\lambda}$  is consistent for  $\beta_0^*$  for  $\lambda = O(\lambda_{\mathcal{O}})$ :

$$\begin{aligned} \arg \min_{\dot{\beta}_{\mathcal{M}}, \dot{\beta}_{-\mathcal{M}}} \Psi_T(\dot{\beta}_{\mathcal{M}}, \dot{\beta}_{-\mathcal{M}} | \lambda) &=: (\hat{\beta}'_{\lambda, \mathcal{M}}, \hat{\beta}'_{\lambda, -\mathcal{M}})' \\ &\xrightarrow{p} (\beta_{\mathcal{M}}^*, \mathbf{0})' \tag{A33} \\ &= \arg \min_{\dot{\beta}_{\mathcal{M}}, \dot{\beta}_{-\mathcal{M}}} \Psi_0(\dot{\beta}_{\mathcal{M}}, \dot{\beta}_{-\mathcal{M}} | \lambda). \end{aligned}$$

- (b) We next analyse the properties of  $\lambda_{0, \rho^* \sim c/T}$  as  $T \rightarrow \infty$ . Note that  $\lim_{T \rightarrow \infty} \rho^* = 0$  for  $\rho^* \sim c/T$ . Therefore, by definition of  $\lambda_{\mathcal{O}}$ ,

$$\lambda_{0, \rho^* \sim c/T} = o_p(\lambda_{\mathcal{O}}), \tag{A34}$$

i.e., sequences  $\lambda_{0, \rho^* \sim c/T}$  are asymptotically restricted to the interval  $[0, \lambda_{\mathcal{O}}]$ . By (A33), the coefficients  $\beta^*$  hence are consistently estimated at all possible activation thresholds of  $y_{t-1}$ ,

$$\hat{\beta}_{\lambda} \xrightarrow{p} \beta_0^* \quad \forall \lambda = \lambda_{0, \rho^* \sim c/T}. \tag{A35}$$

To analyse the asymptotic behaviour of  $\lambda_{0, \rho^* \sim c/T}$ , note that  $\rho^* = \phi(1)^{-1} c/T$  under the local parameterisation  $\varrho^* = 1 + c/T$ ,  $c \in (-\infty, 0]$ , cf. the discussion preceding Theorem 1 in Aylar et al. (2019). Appealing to Equation (8) on page 7,

we now have

$$\lambda_{0,\rho^*} = \underbrace{|\hat{\rho}|^{\gamma_1}}_{=A_T} \left| \underbrace{\sum_t y_{t-1} \varepsilon_{p,t}}_{=B_{T,\lambda}} + \underbrace{\sum_{j=1}^p (\delta_j^* - \hat{\delta}_{\lambda,j}) \sum_t y_{t-1} \Delta y_{t-j}}_{=C_{T,\lambda}} + \phi(1)^{-1} c/T \underbrace{\sum_t y_{t-1}^2}_{=:D_T} \right| \quad (\text{A36})$$

By substituting and rearranging, we get

$$\begin{aligned} \tau_{\gamma_1} &= T^{\gamma_1-1} \lambda_{0,\rho^*} \\ &= |TA_T|^{\gamma_1} |T^{-1}B_{T,\lambda} + T^{-1}C_{T,\lambda} + \phi(1)^{-1}c \cdot T^{-2}D_T| \end{aligned} \quad (\text{A37})$$

We next consider the individual components of (A37). By results of Aylar et al. (2019) and Hansen (1995),

$$TA_T \xrightarrow{d} A := \phi(1)^{-1} \left( \frac{\int_0^1 W_c(r) dW(r)}{\int_0^1 W_c(r)^2 dr} + c \right), \quad (\text{A38})$$

$$T^{-2}D_T \xrightarrow{d} D := \sigma^2 \phi(1)^2 \int_0^1 W_c(r)^2 dr, \quad (\text{A39})$$

with the Ornstein-Uhlenbeck process  $W_c(r)$  defined by the stochastic differential equation  $dW_c(r) = cW_c(r)dr + dW(r)$ ,  $r \in [0, 1]$ , with zero starting value.

The components  $B_{T,\lambda}$  and  $C_{T,\lambda}$  depend on the adaptive Lasso solution  $\hat{\beta}_\lambda$ . Since consistency of  $\hat{\beta}_\lambda$  at  $\lambda = \lambda_{0,\rho^* \sim c/T}$  is ensured per (A35), we have  $\varepsilon_{p,t} \xrightarrow{p} \varepsilon_t$  by Aylar et al. (2019) so that, by Hansen (1995),

$$T^{-1}B_{T,\lambda} \xrightarrow{d} B := \sigma^2 \phi(1) \int_0^1 W_c(r) dW(r). \quad (\text{A40})$$

Turning to  $C_{T,\lambda}$ , we note that

$$T^{-1} \sum_t y_{t-1} \Delta y_{t-j} \Big|_{c \in (-\infty, 0]} = O_p(1) \quad \forall j \geq 0,$$

and further that (A35) implies

$$\delta_j^* - \hat{\delta}_{j,\lambda} \xrightarrow{p} 0, \quad j = 1, \dots, p \quad \forall \lambda = \lambda_{0,\rho^* \sim c/T}.$$

By Slutsky's Theorem, we hence have

$$T^{-1}C_{T,\lambda} \xrightarrow{p} 0 \quad \forall \lambda = \lambda_0, \rho^* \sim c/T. \quad (\text{A41})$$

Applying the results (A38) – (A41) and Slutsky's Theorem to (A37) shows that

$$\tau_{\gamma_1} \Big|_{c \in (-\infty, 0]} = O_p(1) \quad \text{and} \quad \lambda_0, \rho^* \sim c/T \Big|_{c \in (-\infty, 0]} = O_p(T^{1-\gamma_1}). \quad (\text{A42})$$

(c) To derive the limiting r.v. in (13), note that

$$\int_0^1 W_c(r) dW(r) = \frac{1}{2}(W_c(1)^2 - 1) - c \cdot \int_0^1 W_c(r)^2 dr, \quad (\text{A43})$$

see Phillips (1987). Using this result, it is straightforward to establish that

$$A = \phi(1)^{-1} \frac{W_c(1)^2 - 1}{2 \int_0^1 W_c(r)^2 dr}, \quad B + \phi(1)^{-1} c \cdot D = \frac{1}{2} \phi(1) \sigma^2 (W_c(1)^2 - 1). \quad (\text{A44})$$

Using the representations (A44) and applying the continuous mapping theorem (CMT) obtains

$$\begin{aligned} \tau_{\gamma_1} &\xrightarrow{d} |A|^{\gamma_1} |B + \phi(1)^{-1} c \cdot D| \\ &= \left| \phi(1)^{-1} \frac{W_c(1)^2 - 1}{2 \int_0^1 W_c(r)^2 dr} \right|^{\gamma_1} \left| \frac{1}{2} \phi(1) \sigma^2 (W_c(1)^2 - 1) \right|, \end{aligned}$$

which completes the proof of part 1.

2. Result 2 follows directly from the argument of part 2 of Proposition 2 of Arnold and Reinschlüssel (2023). ■

***Proof of Corollary 1.***

1. The exposition in Herwartz and Siedenburg (2010) shows  $J_\alpha$  to converge to a positively-bounded r.v.  $J_{\alpha,c}$  under Assumptions 1 and 2. The result then follows from the CMT.
2. The result follows directly from part 2 of Proposition 2 in Arnold and Reinschlüssel (2023). ■



## B Details on the computation of the penalty weights

**Algorithm 1** ( $\check{w}_1$ ).

1. After adjusting  $y_t$  for the deterministic component  $d_t$ , estimate the LRV  $\omega^2$  using model (3) by

$$\widehat{\omega}_{\text{AR}}^2(k) = \frac{\widehat{\sigma}_k^2}{(1 - \sum_{j=1}^k \widehat{\delta}_j)^2}, \quad \widehat{\sigma}_k^2 = (T - k)^{-1} \sum_{t=k+1}^T \widehat{e}_{t,k}^2$$

for suitable  $k$ .

2. Scale  $y_t$  by  $\widehat{\omega}_{\text{AR}}(k)^{-1}$ .
3. For some fixed  $\alpha \in (0, .5)$ , obtain the range statistic  $J_\alpha := \left| \widehat{\zeta}_{1-\alpha/2}^{(r)} - \widehat{\zeta}_{\alpha/2}^{(r)} \right|$  with  $\widehat{\zeta}_\alpha^{(r)}$  the  $\alpha$  quantile of simulated OLS estimates  $\widehat{\zeta}^{(r)}$ , in the model

$$y_t = \mu^{(r)} + \varsigma^{(r)}t + \zeta^{(r)}x_t^{(r)} + \nu_t^{(r)}, \quad r = 1, \dots, R,$$

where  $x_t^{(r)}$  is a Gaussian random walk with zero initial condition.

4. Compute  $\check{w}_1 := |\widehat{\rho}/J_\alpha|$  with  $\widehat{\rho}$  the OLS estimator of  $\rho^*$  in model (3), adjusted for  $d_t$  as in step 1. ■

# C Additional Figures

Figure C1: Location of the groundwater measurement stations in NRW, Germany



*Notes:* Black outlines show the borders of the Federal Republic of Germany. The federal state of North Rhine-Westphalia is shaded grey.

## D Additional simulation results

Table D1: Critical values of activation knot tests under FD trend adjustment

$T$	$\tau$			$\check{\tau}$		
	1%	5%	10%	1%	5%	10%
<i>constant</i>						
50	7.40	4.28	3.06	13.21	5.32	3.08
75	7.25	4.23	3.02	13.55	5.40	3.12
100	7.18	4.21	3.02	13.72	5.49	3.17
150	7.12	4.19	3.01	14.02	5.59	3.22
250	7.08	4.16	2.99	13.98	5.58	3.21
500	6.97	4.15	2.98	13.96	5.62	3.23
1000	6.95	4.15	2.98	13.93	5.65	3.23
<i>linear trend</i>						
50	10.97	7.22	5.65	20.15	10.49	7.24
75	10.65	7.07	5.56	20.85	10.85	7.51
100	10.51	7.03	5.55	21.41	11.08	7.65
150	10.37	6.94	5.49	21.68	11.21	7.72
250	10.21	6.90	5.47	21.84	11.31	7.83
500	10.15	6.85	5.46	22.06	11.41	7.88
1000	10.13	6.87	5.44	22.25	11.51	7.93

*Notes:* Critical values are computed based on the adaptive Lasso solution to (3) with  $d_t = 0$  and  $p = 0$ .  $\check{\tau}$  is computed using  $J_\alpha$  with  $\alpha = .1$  and  $\sigma^2$  estimated by  $\widehat{\sigma}^2$ . Data adjusted for a constant are obtained as  $y_t^{\text{FD}} = y_t - y_1$ . Data adjusted for a linear time trend are obtained as  $y_t^{\text{FD}} = y_t - y_1 - t/T(y_T - y_1)$ .  $5 \cdot 10^5$  replications.

Table D2: Empirical size: AR errors – no adjustment

$T$	$\varphi$	$\tau$	$\check{\tau}$	$ADF^{\text{GLS}}$	$MZ_t$	$J_\alpha$
50		.056	.031	.039	.004	.019
75		.054	.035	.040	.003	.024
100		.052	.033	.040	.005	.024
150	-.8	.051	.042	.043	.010	.032
250		.049	.041	.044	.017	.031
500		.055	.049	.048	.029	.041
1000		.051	.049	.050	.038	.045
50		.064	.045	.046	.014	.024
75		.056	.039	.037	.010	.021
100		.061	.044	.046	.019	.030
150	-.4	.054	.044	.044	.019	.029
250		.050	.044	.043	.024	.035
500		.051	.049	.050	.034	.041
1000		.048	.050	.050	.041	.043
50		.051	.028	.045	.014	.023
75		.045	.026	.042	.014	.020
100		.042	.028	.044	.016	.020
150	0	.044	.035	.046	.020	.027
250		.044	.036	.042	.022	.030
500		.052	.045	.050	.036	.037
1000		.045	.043	.046	.037	.042
50		.066	.018	.042	.012	.014
75		.062	.025	.044	.014	.020
100		.053	.028	.041	.021	.025
150	.4	.050	.033	.044	.022	.028
250		.046	.037	.041	.028	.031
500		.045	.037	.044	.032	.035
1000		.051	.050	.049	.043	.046
50		.083	.022	.051	.034	.022
75		.069	.024	.049	.025	.021
100		.055	.026	.043	.026	.022
150	.8	.051	.033	.044	.024	.026
250		.049	.037	.045	.028	.030
500		.051	.042	.046	.035	.038
1000		.049	.048	.052	.045	.043

Notes: DGP (27) with  $c = 0$  and  $v_t = \varphi v_{t-1} + \epsilon_t$ ,  $\epsilon_t \sim i.i.d. N(0, 1)$ . Model (3) with  $d_t = 0$  and  $p = \lfloor 12 \cdot (T/100)^{-25} \rfloor$ .  $\tau$  and  $\check{\tau}$  are activation knot tests based on FD-adjustment, if applicable.  $ADF^{\text{GLS}}$  and  $MZ_t$  are the modified augmented Dickey-Fuller (Elliott et al., 1996) and Phillips-Perron  $Z_t$  test (Ng & Perron, 2001) with GLS-adjusted data, if applicable.  $J_\alpha$  is computed as stated in Herwartz and Siedenburg (2010) using OLS-adjusted data, if applicable. The LRV is estimated as detailed in Section 4.2. 5000 replications.

Table D3: Empirical size: AR errors – demeaning

$T$	$\varphi$	$\tau$	$\check{\tau}$	ADF <sup>GLS</sup>	MZ <sub><math>t</math></sub>	$J_\alpha$
50		.063	.057	.027	.006	.048
75		.054	.056	.031	.007	.045
100		.051	.049	.030	.007	.043
150	-.8	.046	.044	.031	.013	.043
250		.052	.054	.045	.031	.045
500		.046	.046	.041	.034	.045
1000		.048	.049	.049	.044	.045
50		.078	.077	.039	.040	.059
75		.063	.061	.031	.033	.044
100		.056	.063	.037	.036	.047
150	-.4	.058	.057	.039	.039	.047
250		.051	.051	.041	.041	.044
500		.052	.053	.046	.045	.048
1000		.048	.049	.046	.046	.047
50		.047	.047	.037	.040	.042
75		.040	.038	.030	.032	.035
100		.045	.047	.037	.038	.047
150	0	.052	.049	.046	.049	.044
250		.046	.046	.043	.043	.049
500		.051	.046	.049	.049	.049
1000		.055	.055	.054	.055	.053
50		.037	.021	.012	.038	.027
75		.038	.029	.026	.041	.036
100		.041	.031	.028	.043	.040
150	.4	.046	.040	.038	.050	.042
250		.049	.046	.045	.052	.044
500		.050	.043	.045	.047	.045
1000		.047	.049	.044	.046	.046
50		.053	.042	.030	.119	.059
75		.050	.037	.032	.083	.042
100		.050	.037	.035	.064	.037
150	.8	.048	.041	.040	.057	.037
250		.047	.045	.043	.053	.041
500		.046	.045	.046	.048	.039
1000		.051	.050	.050	.052	.046

Notes: DGP (27) with  $c = 0$  and  $v_t = \varphi v_{t-1} + \epsilon_t$ ,  $\epsilon_t \sim i.i.d. N(0, 1)$ . Model (3) with  $d_t = 0$  and  $p = \lfloor 12 \cdot (T/100)^{.25} \rfloor$ . Data are adjusted for a constant. See Table D2 for further details. 5000 replications.

Table D4: Empirical size: AR errors – detrending

$T$	$\varphi$	$\tau$	$\check{\tau}$	ADF <sup>GLS</sup>	MZ <sub><math>t</math></sub>	$J_\alpha$
50		.073	.078	.025	.003	.070
75		.068	.070	.028	.002	.062
100		.056	.061	.025	.002	.048
150	-.8	.050	.052	.026	.004	.050
250		.047	.047	.032	.011	.050
500		.047	.048	.037	.021	.050
1000		.050	.050	.044	.032	.048
50		.117	.104	.040	.044	.072
75		.099	.098	.032	.035	.070
100		.080	.080	.030	.031	.054
150	-.4	.073	.070	.032	.031	.045
250		.064	.066	.035	.035	.046
500		.047	.049	.037	.037	.047
1000		.051	.052	.044	.043	.048
50		.040	.037	.029	.031	.045
75		.040	.041	.033	.034	.039
100		.044	.042	.037	.040	.044
150	0	.044	.043	.034	.036	.045
250		.043	.043	.036	.036	.041
500		.044	.039	.035	.035	.042
1000		.049	.050	.048	.049	.051
50		.008	.007	.003	.035	.014
75		.015	.014	.012	.045	.023
100		.025	.024	.022	.051	.036
150	.4	.034	.032	.030	.049	.043
250		.038	.036	.032	.044	.045
500		.047	.045	.044	.051	.047
1000		.049	.045	.042	.046	.044
50		.038	.038	.028	.238	.068
75		.042	.033	.032	.143	.041
100		.040	.030	.031	.103	.032
150	.8	.045	.036	.037	.077	.038
250		.045	.038	.040	.059	.031
500		.045	.043	.042	.052	.036
1000		.043	.044	.043	.049	.043

Notes: DGP (27) with  $c = 0$  and  $v_t = \varphi v_{t-1} + \epsilon_t$ ,  $\epsilon_t \sim i.i.d. N(0, 1)$ . Model (3) with  $d_t = 0$  and  $p = \lfloor 12 \cdot (T/100)^{.25} \rfloor$ . Data are adjusted for a linear time trend. See Table D2 for further details. 5000 replications.

Table D5: Size-adjusted local power: AR errors – no adjustment

$T$	$\varphi$	$\tau$	$\check{\tau}$	ADF <sup>GLS</sup>	MZ <sub><math>t</math></sub>	$J_\alpha$
50		.474	.608	.374	.518	.603
75		.466	.605	.408	.569	.607
100		.468	.617	.439	.585	.592
150	-.8	.460	.554	.478	.568	.519
250		.489	.573	.503	.559	.532
500		.438	.505	.503	.518	.481
1000		.458	.506	.504	.511	.459
50		.485	.578	.351	.556	.573
75		.501	.596	.431	.630	.591
100		.456	.577	.429	.608	.553
150	-.4	.474	.564	.483	.601	.551
250		.487	.560	.510	.597	.500
500		.469	.510	.503	.524	.463
1000		.462	.496	.506	.513	.461
50		.404	.605	.414	.661	.601
75		.475	.610	.462	.682	.612
100		.450	.616	.474	.650	.600
150	0	.471	.568	.474	.606	.550
250		.470	.573	.509	.603	.535
500		.433	.522	.499	.521	.493
1000		.474	.518	.529	.531	.477
50		.138	.479	.271	.537	.536
75		.237	.505	.355	.564	.532
100		.319	.509	.420	.544	.507
150	.4	.383	.548	.462	.602	.541
250		.451	.553	.542	.604	.499
500		.478	.548	.533	.548	.502
1000		.431	.478	.503	.506	.438
50		.110	.360	.203	.310	.309
75		.192	.400	.273	.439	.401
100		.269	.457	.335	.453	.416
150	.8	.331	.465	.406	.476	.452
250		.396	.473	.453	.473	.446
500		.408	.500	.479	.492	.447
1000		.418	.468	.457	.464	.426

Notes: DGP (27) with  $c = -7$  and  $v_t = \varphi v_{t-1} + \epsilon_t$ ,  $\epsilon_t \sim i.i.d. N(0, 1)$ . Model (3) with  $d_t = 0$  and  $p = \lfloor 12 \cdot (T/100)^{.25} \rfloor$ . See Table D2 for further details. 5000 replications.

Table D6: Size-adjusted local power: AR errors – demeaning

$T$	$\varphi$	$\tau$	$\check{\tau}$	ADF <sup>GLS</sup>	MZ <sub><math>t</math></sub>	$J_\alpha$
50		.185	.228	.225	.191	.230
75		.203	.239	.228	.206	.234
100		.213	.257	.238	.217	.252
150	-.8	.234	.295	.279	.268	.272
250		.218	.256	.244	.231	.255
500		.263	.308	.321	.312	.268
1000		.299	.347	.328	.327	.301
50		.217	.246	.223	.216	.214
75		.239	.277	.264	.249	.251
100		.234	.248	.241	.235	.231
150	-.4	.234	.279	.265	.264	.255
250		.238	.282	.269	.277	.248
500		.244	.294	.296	.298	.253
1000		.309	.363	.357	.363	.278
50		.217	.263	.272	.271	.236
75		.251	.312	.316	.311	.273
100		.209	.247	.259	.253	.230
150	0	.199	.252	.243	.233	.236
250		.245	.298	.291	.286	.253
500		.251	.320	.293	.297	.266
1000		.268	.317	.306	.307	.259
50		.091	.170	.176	.130	.159
75		.144	.229	.227	.205	.202
100		.183	.247	.263	.248	.218
150	.4	.188	.260	.261	.243	.243
250		.211	.270	.261	.252	.252
500		.236	.310	.296	.291	.266
1000		.304	.340	.354	.354	.292
50		.099	.145	.163	.069	.082
75		.125	.178	.176	.137	.148
100		.133	.196	.193	.164	.176
150	.8	.162	.215	.207	.201	.183
250		.205	.242	.246	.234	.207
500		.250	.299	.286	.295	.265
1000		.274	.326	.318	.314	.275

Notes: DGP (27) with  $c = -7$  and  $v_t = \varphi v_{t-1} + \epsilon_t$ ,  $\epsilon_t \sim i.i.d. N(0, 1)$ . Model (3) with  $d_t = 0$  and  $p = \lfloor 12 \cdot (T/100)^{.25} \rfloor$ . Data are adjusted for a constant. See Table D2 for further details. 5000 replications.



Table D7: Size-adjusted local power: AR errors – detrending

$T$	$\varphi$	$\tau$	$\check{\tau}$	ADF <sup>GLS</sup>	MZ <sub><math>t</math></sub>	$J_\alpha$
50		.216	.263	.269	.176	.307
75		.241	.277	.309	.212	.305
100		.268	.312	.310	.252	.346
150	-.8	.300	.335	.331	.288	.315
250		.318	.360	.329	.332	.313
500		.363	.389	.397	.392	.334
1000		.372	.409	.408	.406	.355
50		.315	.343	.262	.245	.302
75		.289	.310	.276	.281	.271
100		.324	.363	.333	.322	.323
150	-.4	.332	.365	.356	.333	.342
250		.339	.371	.367	.369	.351
500		.384	.404	.374	.374	.336
1000		.369	.388	.394	.396	.348
50		.376	.400	.360	.376	.333
75		.364	.385	.382	.381	.349
100		.351	.374	.345	.352	.319
150	0	.358	.371	.367	.366	.316
250		.367	.401	.385	.394	.352
500		.376	.423	.409	.408	.348
1000		.371	.388	.390	.385	.333
50		.190	.201	.188	.056	.176
75		.178	.194	.151	.108	.178
100		.226	.249	.216	.181	.215
150	.4	.281	.296	.294	.293	.278
250		.342	.352	.349	.348	.291
500		.323	.341	.328	.331	.306
1000		.362	.399	.396	.396	.358
50		.083	.070	.072	.018	.044
75		.136	.150	.146	.080	.129
100		.180	.188	.181	.135	.163
150	.8	.208	.219	.214	.184	.175
250		.251	.279	.262	.251	.260
500		.307	.318	.308	.299	.291
1000		.370	.376	.370	.361	.322

Notes: DGP (27) with  $c = -13.5$  and  $v_t = \varphi v_{t-1} + \epsilon_t$ ,  $\epsilon_t \sim i.i.d. N(0, 1)$ . Model (3) with  $d_t = 0$  and  $p = \lfloor 12 \cdot (T/100)^{.25} \rfloor$ . Data are adjusted for a linear time trend. See Table D2 for further details. 5000 replications.

Table D8: Empirical size: MA errors – no adjustment

$T$	$\vartheta$	$\tau$	$\check{\tau}$	ADF <sup>GLS</sup>	MZ <sub><math>t</math></sub>	$J_\alpha$
50		.240	.187	.071	.041	.083
75		.242	.181	.062	.023	.077
100		.240	.179	.064	.022	.073
150	-.8	.226	.176	.069	.017	.072
250		.205	.163	.075	.015	.066
500		.161	.136	.067	.023	.060
1000		.132	.120	.075	.045	.064
50		.082	.061	.054	.022	.031
75		.073	.055	.047	.017	.029
100		.069	.055	.044	.022	.033
150	-.4	.076	.065	.054	.025	.038
250		.065	.058	.047	.031	.036
500		.072	.068	.057	.043	.050
1000		.056	.056	.046	.038	.046
50		.060	.025	.043	.015	.019
75		.047	.025	.038	.014	.017
100		.057	.037	.047	.022	.029
150	.4	.047	.036	.038	.021	.033
250		.053	.044	.046	.027	.035
500		.051	.046	.045	.031	.041
1000		.048	.045	.046	.038	.040
50		.069	.028	.040	.019	.022
75		.065	.034	.042	.020	.023
100		.066	.038	.042	.021	.028
150	.8	.057	.036	.039	.025	.029
250		.060	.048	.043	.032	.039
500		.051	.048	.042	.038	.043
1000		.048	.047	.045	.043	.043

Notes: DGP (27) with  $c = 0$  and  $v_t = \vartheta\epsilon_{t-1} + \epsilon_t$ ,  $\epsilon_t \sim i.i.d. N(0, 1)$ . Model (3) with  $d_t = 0$  and  $p = \lfloor 12 \cdot (T/100)^{-25} \rfloor$ . See Table D2 for further details. 5000 replications.

Table D9: Empirical size: MA errors – demeaning

$T$	$\vartheta$	$\tau$	$\check{\tau}$	ADF <sup>GLS</sup>	MZ <sub><math>t</math></sub>	$J_\alpha$
50		.370	.372	.207	.177	.291
75		.298	.291	.131	.093	.202
100		.275	.263	.103	.059	.162
150	-.8	.252	.237	.081	.033	.124
250		.217	.203	.068	.021	.085
500		.170	.163	.071	.027	.085
1000		.139	.134	.070	.040	.072
50		.117	.119	.067	.066	.082
75		.109	.109	.057	.056	.073
100		.092	.093	.045	.045	.060
150	-.4	.090	.094	.053	.052	.062
250		.073	.076	.050	.049	.053
500		.063	.066	.049	.050	.052
1000		.061	.063	.049	.049	.049
50		.046	.028	.015	.035	.033
75		.039	.036	.023	.042	.035
100		.048	.041	.030	.042	.046
150	.4	.051	.047	.035	.044	.047
250		.052	.052	.041	.048	.045
500		.053	.051	.047	.049	.048
1000		.049	.047	.049	.051	.047
50		.059	.045	.017	.059	.042
75		.055	.043	.018	.046	.035
100		.047	.044	.018	.045	.044
150	.8	.047	.045	.024	.044	.043
250		.053	.054	.034	.051	.046
500		.051	.047	.041	.050	.046
1000		.055	.056	.049	.055	.052

Notes: DGP (27) with  $c = 0$  and  $v_t = \vartheta\epsilon_{t-1} + \epsilon_t$ ,  $\epsilon_t \sim i.i.d. N(0, 1)$ . Model (3) with  $d_t = 0$  and  $p = \lfloor 12 \cdot (T/100)^{-25} \rfloor$ . Data are adjusted for a constant. See Table D2 for further details. 5000 replications.

Table D10: Empirical size: MA errors – detrending

$T$	$\vartheta$	$\tau$	$\check{\tau}$	ADF <sup>GLS</sup>	MZ <sub><math>t</math></sub>	$J_\alpha$
50		.558	.582	.359	.348	.498
75		.502	.503	.244	.216	.387
100		.442	.432	.176	.132	.300
150	-.8	.377	.353	.102	.054	.218
250		.348	.311	.074	.021	.152
500		.289	.250	.059	.010	.108
1000		.232	.194	.072	.014	.085
50		.204	.184	.097	.108	.132
75		.176	.152	.061	.072	.099
100		.168	.149	.057	.061	.086
150	-.4	.135	.119	.046	.050	.071
250		.117	.104	.043	.045	.059
500		.101	.089	.041	.044	.053
1000		.081	.073	.048	.049	.050
50		.014	.011	.004	.030	.018
75		.028	.027	.013	.042	.037
100		.034	.030	.020	.046	.037
150	.4	.047	.046	.034	.057	.055
250		.051	.048	.032	.046	.045
500		.048	.046	.033	.042	.042
1000		.046	.049	.039	.045	.048
50		.033	.027	.005	.069	.033
75		.047	.042	.007	.060	.039
100		.044	.043	.009	.056	.040
150	.8	.043	.043	.011	.055	.042
250		.044	.046	.021	.051	.050
500		.051	.056	.033	.063	.056
1000		.051	.053	.037	.054	.053

Notes: DGP (27) with  $c = 0$  and  $v_t = \vartheta\epsilon_{t-1} + \epsilon_t$ ,  $\epsilon_t \sim i.i.d. N(0, 1)$ . Model (3) with  $d_t = 0$  and  $p = \lfloor 12 \cdot (T/100)^{-25} \rfloor$ . Data are adjusted for a linear time trend. See Table D2 for further details. 5000 replications.

Table D11: Size-adjusted local power: MA errors – no adjustment

$T$	$\vartheta$	$\tau$	$\check{\tau}$	ADF <sup>GLS</sup>	MZ <sub><math>t</math></sub>	$J_\alpha$
50		.643	.618	.453	.471	.564
75		.646	.639	.413	.400	.570
100		.623	.585	.373	.355	.535
150	-.8	.593	.584	.415	.377	.522
250		.561	.565	.430	.373	.509
500		.562	.552	.497	.486	.503
1000		.462	.464	.468	.431	.418
50		.558	.605	.354	.499	.564
75		.586	.615	.415	.559	.570
100		.602	.620	.459	.578	.565
150	-.4	.522	.557	.438	.565	.520
250		.563	.583	.526	.560	.538
500		.484	.482	.472	.496	.450
1000		.520	.529	.544	.559	.470
50		.210	.482	.269	.519	.514
75		.357	.560	.377	.596	.572
100		.352	.513	.393	.576	.516
150	.4	.439	.536	.454	.593	.524
250		.439	.521	.472	.558	.498
500		.454	.534	.507	.532	.474
1000		.450	.528	.520	.540	.483
50		.231	.466	.218	.427	.485
75		.274	.469	.280	.458	.479
100		.283	.462	.296	.446	.473
150	.8	.348	.516	.385	.518	.489
250		.365	.457	.408	.475	.437
500		.432	.485	.479	.477	.452
1000		.441	.493	.491	.487	.455

Notes: DGP (27) with  $c = -7$  and  $v_t = \vartheta\epsilon_{t-1} + \epsilon_t$ ,  $\epsilon_t \sim i.i.d. N(0, 1)$ . Model (3) with  $d_t = 0$  and  $p = \lfloor 12 \cdot (T/100)^{-25} \rfloor$ . See Table D2 for further details. 5000 replications.

Table D12: Size-adjusted local power: MA errors – demeaning

$T$	$\vartheta$	$\tau$	$\check{\tau}$	ADF <sup>GLS</sup>	MZ <sub><math>t</math></sub>	$J_\alpha$
50		.163	.204	.197	.195	.222
75		.202	.238	.208	.212	.229
100		.185	.206	.170	.171	.207
150	-.8	.184	.213	.173	.148	.211
250		.210	.214	.177	.160	.245
500		.220	.235	.224	.197	.242
1000		.286	.302	.287	.274	.262
50		.231	.254	.214	.209	.235
75		.231	.236	.214	.208	.208
100		.246	.266	.239	.234	.239
150	-.4	.234	.246	.231	.227	.221
250		.272	.280	.264	.261	.248
500		.295	.318	.293	.293	.278
1000		.334	.369	.354	.353	.303
50		.101	.193	.196	.152	.185
75		.183	.235	.216	.193	.203
100		.180	.245	.243	.235	.213
150	.4	.193	.250	.251	.250	.209
250		.222	.258	.256	.249	.243
500		.227	.291	.284	.284	.241
1000		.283	.351	.323	.323	.281
50		.112	.170	.172	.100	.152
75		.150	.212	.210	.162	.193
100		.181	.221	.206	.187	.180
150	.8	.185	.233	.225	.212	.217
250		.188	.237	.232	.220	.231
500		.224	.298	.273	.267	.253
1000		.260	.300	.297	.293	.260

Notes: DGP (27) with  $c = -7$  and  $v_t = \vartheta\epsilon_{t-1} + \epsilon_t$ ,  $\epsilon_t \sim i.i.d. N(0, 1)$ . Model (3) with  $d_t = 0$  and  $p = \lfloor 12 \cdot (T/100)^{-25} \rfloor$ . Data are adjusted for a constant. See Table D2 for further details. 5000 replications.

Table D13: Size-adjusted local power: MA errors – detrending

$T$	$\vartheta$	$\tau$	$\check{\tau}$	ADF <sup>GLS</sup>	MZ <sub><math>t</math></sub>	$J_\alpha$
50		.192	.255	.271	.137	.302
75		.222	.283	.288	.279	.329
100		.237	.294	.274	.268	.317
150	-.8	.224	.271	.246	.237	.292
250		.228	.263	.215	.183	.274
500		.260	.304	.268	.219	.326
1000		.282	.326	.303	.251	.328
50		.294	.334	.247	.269	.319
75		.287	.322	.264	.258	.301
100		.281	.306	.263	.251	.303
150	-.4	.316	.352	.303	.288	.313
250		.336	.372	.317	.318	.327
500		.340	.390	.373	.364	.355
1000		.391	.417	.398	.400	.365
50		.254	.288	.316	.140	.261
75		.202	.224	.204	.121	.199
100		.242	.262	.214	.179	.244
150	.4	.283	.284	.252	.252	.246
250		.322	.338	.313	.317	.300
500		.361	.383	.368	.355	.325
1000		.382	.401	.383	.381	.333
50		.158	.182	.183	.042	.147
75		.192	.225	.215	.121	.206
100		.236	.261	.248	.161	.227
150	.8	.261	.291	.261	.201	.248
250		.292	.316	.301	.258	.260
500		.289	.311	.281	.270	.282
1000		.334	.359	.352	.342	.314

Notes: DGP (27) with  $c = -13.5$  and  $v_t = \vartheta\epsilon_{t-1} + \epsilon_t$ ,  $\epsilon_t \sim i.i.d. N(0, 1)$ . Model (3) with  $d_t = 0$  and  $p = \lfloor 12 \cdot (T/100)^{.25} \rfloor$ . Data are adjusted for a linear time trend. See Table D2 for further details. 5000 replications.

## References

- Adamek, R., Smeeke, S., & Wilms, I. (2023). Lasso inference for high-dimensional time series. *Journal of Econometrics*, *235*(2), 1114–1143.
- Aylar, E., Smeeke, S., & Westerlund, J. (2019). Lag truncation and the local asymptotic distribution of the ADF test for a unit root. *Statistical Papers*, *60*(6), 2109–2118.
- Belloni, A., Chernozhukov, V., & Hansen, C. (2013). Inference on treatment effects after selection among high-dimensional controls. *Review of Economic Studies*, *81*(2), 608–650.
- Caner, M., & Knight, K. (2013). An alternative to unit root tests: Bridge estimators differentiate between nonstationary versus stationary models and select optimal lag. *Journal of Statistical Planning and Inference*, *143*(4), 691–715.
- Chang, Y., & Park, J. (2002). On the asymptotics of ADF tests for unit roots. *Econometric Reviews*, *21*(4), 431–447.
- Chernozhukov, V., Chetverikov, D., Kato, K., & Koike, Y. (2023). High-dimensional data bootstrap. *Annual Review of Statistics and Its Application*, *10*(1), 427–449.
- Dickey, D. A., & Fuller, W. A. (1979). Distribution of the estimators for autoregressive time series with a unit root. *Journal of the American Statistical Association*, *74*(366a), 427–431.
- Dickey, D. A., & Fuller, W. A. (1981). Likelihood ratio statistics for autoregressive time series with a unit root. *Econometrica*, *49*(4), 1057–1072.
- Efron, B., Hastie, T., Johnstone, I., & Tibshirani, R. (2004). Least angle regression. *The Annals of Statistics*, *32*(2), 407–499.
- Elliott, G., Rothenberg, T. J., & Stock, J. H. (1996). Efficient tests for an autoregressive unit root. *Econometrica*, *64*(4), 813–836.
- Fu, W., & Knight, K. (2000). Asymptotics for lasso-type estimators. *The Annals of Statistics*, *28*(5), 1356–1378.
- Hansen, B. E. (1995). Rethinking the Univariate Approach to Unit Root Testing: Using Covariates to Increase Power. *Econometric Theory*, *11*(5), 1148–1171.



- Hastie, T., & Efron, B. (2022). *Lars: Least angle regression, lasso and forward stagewise* [R package version 1.3].
- Hecq, A., Margaritella, L., & Smeekes, S. (2023). Granger causality testing in high-dimensional VARs: A post-double-selection procedure. *Journal of Financial Econometrics*, *21*(3), 915–958.
- Herwartz, H., & Siedenburg, F. (2010). A new approach to unit root testing. *Computational Economics*, *36*(4), 365–384.
- Hsu, N.-J., Hung, H.-L., & Chang, Y.-M. (2008). Subset selection for vector autoregressive processes using lasso. *Computational Statistics & Data Analysis*, *52*(7), 3645–3657.
- Kock, A. B. (2016). Consistent and conservative model selection with the adaptive lasso in stationary and nonstationary autoregressions. *Econometric Theory*, *32*(1), 243–259.
- Koo, B., Anderson, H. M., Seo, M. H., & Yao, W. (2020). High-dimensional predictive regression in the presence of cointegration. *Journal of Econometrics*, *219*(2), 456–477.
- LANUV. (2023). *Climate Atlas NRW* [Data on water management and flood protection: groundwater level]. Landesamt für Natur, Umwelt und Verbraucherschutz NRW.
- Lee, J. D., Sun, D. L., Sun, Y., & Taylor, J. E. (2016). Exact post-selection inference, with application to the lasso. *The Annals of Statistics*, *44*(3), 907–927.
- Lee, J. H., Shi, Z., & Gao, Z. (2022). On LASSO for predictive regression. *Journal of Econometrics*, *229*(2), 322–349.
- Liao, Z., & Phillips, P. C. B. (2015). Automated estimation of vector error correction models. *Econometric Theory*, *31*(3), 581–646.
- Medeiros, M., & Mendes, E. (2012). *Estimating High-Dimensional Time Series Models* (tech. rep.).
- Meinshausen, N., Meier, L., & Bühlmann, P. (2009). p-values for high-dimensional regression. *Journal of the American Statistical Association*, *104*(488), 1671–1681.

- Ng, S., & Perron, P. (2001). Lag length selection and the construction of unit root tests with good size and power. *Econometrica*, 69(6), 1519–1554.
- Perron, P., & Ng, S. (1998). An autoregressive spectral density estimator at frequency zero for nonstationarity tests. *Econometric Theory*, 14(5), 560–603.
- Phillips, P. C. B. (1987). Time series regression with a unit root. *Econometrica*, 55(2), 277–301.
- Pötscher, B. M., & Schneider, U. (2009). On the distribution of the adaptive lasso estimator. *Journal of Statistical Planning and Inference*, 139(8), 2775–2790.
- R Core Team. (2023). *R: A language and environment for statistical computing*. R Foundation for Statistical Computing. Vienna, Austria.
- Reinschlüssel, T., & Arnold, M. C. (2024). Information-Enriched Selection of Stationary and Non-Stationary Autoregressions using the Adaptive Lasso. *arXiv:2402.16580*.
- Ren, Y., & Zhang, X. (2010). Subset selection for vector autoregressive processes via adaptive lasso. *Statistics & Probability Letters*, 80(23-24), 1705–1712.
- Said, S. E., & Dickey, D. A. (1984). Testing for unit roots in autoregressive-moving average models of unknown order. *Biometrika*, 71(3), 599–607.
- Scheihing, K., Kübeck, C., & Sütering, U. (2022). GIS-AHP ensembles for multi-actor multi-criteria site selection processes: Application to groundwater management under climate change. *Water*, 14(11), 1793.
- Schmidt, P., & Phillips, P. C. B. (1992). LM tests for a unit root in the presence of deterministic trends. *Oxford Bulletin of Economics and Statistics*, 54(3), 257–287.
- Silverman, B. W. (1986). *Density estimation for statistics and data analysis*. Chapman; Hall.
- Tibshirani, R. (1996). Regression shrinkage and selection via the lasso. *Journal of the Royal Statistical Society: Series B (Methodological)*, 58(1), 267–288.
- Tibshirani, R., Tibshirani, R., Taylor, J., Loftus, J., Reid, S., & Markovic, J. (2019). *Selectiveinference: Tools for post-selection inference* [R package version 1.2.5].

- Tibshirani, R. J., Rinaldo, A., Tibshirani, R., & Wasserman, L. (2018). Uniform asymptotic inference and the bootstrap after model selection. *The Annals of Statistics*, *46*(3), 1255–1287.
- Tibshirani, R. J., Taylor, J., Lockhart, R., & Tibshirani, R. (2016). Exact post-selection inference for sequential regression procedures. *Journal of the American Statistical Association*, *111*(514), 600–620.
- Umweltbundesamt. (2018). *Wasserwirtschaft in Deutschland – Grundlagen, Belastungen, Maßnahmen*.
- Wang, H., Li, G., & Tsai, C.-L. (2007). Regression coefficient and autoregressive order shrinkage and selection via the lasso. *Journal of the Royal Statistical Society Series B: Statistical Methodology*, *69*(1), 63–78.
- Wünsch, A., Liesch, T., & Broda, S. (2022). Deep learning shows declining groundwater levels in germany until 2100 due to climate change. *Nature Communications*, *13*(1).
- Zou, H. (2006). The adaptive lasso and its oracle properties. *Journal of the American Statistical Association*, *101*(476), 1418–1429.